

# Why the Cox–Merz rule and Gleissle mirror relation work: A quantitative analysis using the Wagner integral framework with a fractional Maxwell kernel

Cite as: Phys. Fluids **34**, 033106 (2022); <https://doi.org/10.1063/5.0084478>

Submitted: 06 January 2022 • Accepted: 22 February 2022 • Published Online: 14 March 2022

Published open access through an agreement with Massachusetts Institute of Technology

 Joshua David John Rathinaraj,  Bavand Keshavarz and  Gareth H. McKinley

## COLLECTIONS

Paper published as part of the special topic on [Celebration of Robert Byron Bird \(1924-2020\)](#)

 This paper was selected as an Editor's Pick



## ARTICLES YOU MAY BE INTERESTED IN

[On Oreology, the fracture and flow of “milk's favorite cookie”<sup>®</sup>](#)

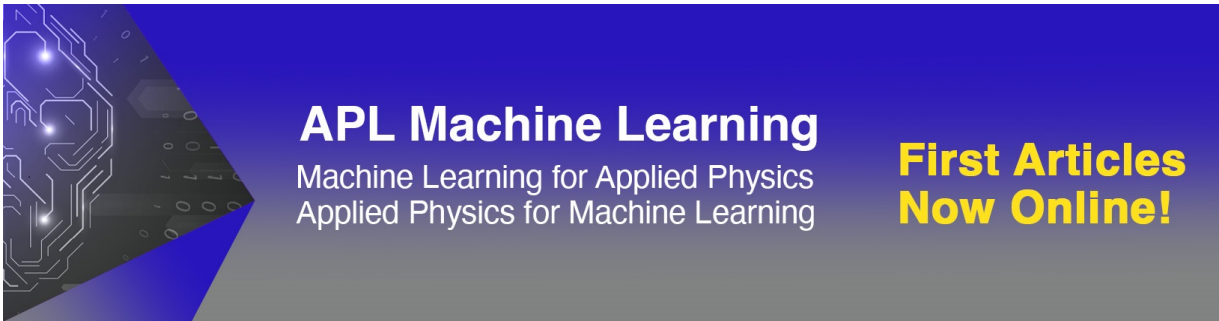
Physics of Fluids **34**, 043107 (2022); <https://doi.org/10.1063/5.0085362>

[Validity of the Cox–Merz rule for concentrated suspensions](#)

Journal of Rheology **47**, 897 (2003); <https://doi.org/10.1122/1.1574020>

[The nonlinear rheology of complex yield stress foods](#)

Physics of Fluids **34**, 023107 (2022); <https://doi.org/10.1063/5.0083974>



**APL Machine Learning**  
Machine Learning for Applied Physics  
Applied Physics for Machine Learning

**First Articles  
Now Online!**

# Why the Cox–Merz rule and Gleissle mirror relation work: A quantitative analysis using the Wagner integral framework with a fractional Maxwell kernel

Cite as: Phys. Fluids **34**, 033106 (2022); doi: 10.1063/5.0084478

Submitted: 6 January 2022 · Accepted: 22 February 2022 ·

Published Online: 14 March 2022



View Online



Export Citation



CrossMark

Joshua David John Rathinaraj,<sup>a)</sup>  Bavand Keshavarz,<sup>b)</sup>  and Gareth H. McKinley<sup>c)</sup> 

## AFFILIATIONS

Hatsopoulos Microfluids Laboratory, Department of Mechanical Engineering, Massachusetts Institute of Technology, Cambridge, Massachusetts 02139, USA

Note: This paper is part of the special topic, Celebration of Robert Byron Bird (1924–2020).

<sup>a)</sup>Electronic mail: [joshuajr@mit.edu](mailto:joshuajr@mit.edu)

<sup>b)</sup>Electronic mail: [bavand@mit.edu](mailto:bavand@mit.edu)

<sup>c)</sup>Author to whom correspondence should be addressed: [gareth@mit.edu](mailto:gareth@mit.edu)

## ABSTRACT

In this work, we mathematically derive the conditions for which empirical rheometric relations such as the Cox–Merz rule and Gleissle mirror relationship are satisfied. We consider the Wagner integral constitutive framework, which is a special limiting case of the Kaye–Bernstein Kearsley Zapas (K-BKZ) constitutive equation to derive analytical expressions for the complex viscosity, the steady shear viscosity, and the transient stress coefficient in the start-up of steady shear. We use a fractional Maxwell liquid model as the linear relaxation modulus or memory kernel within a non-linear integral constitutive framework. This formulation is especially well-suited for describing complex fluids that exhibit a broad relaxation spectrum and can be readily reduced to the canonical Maxwell model for describing viscoelastic liquids that exhibit a single dominant relaxation time. To incorporate the nonlinearities that always become important in real complex fluids at large strain amplitudes, we consider both an exponential damping function as well as a more general damping function. By evaluating analytical expressions for small amplitude oscillatory shear, steady shear, and the start-up of steady shear using these different damping functions, we show that neither the Cox–Merz rule nor the Gleissle mirror relation can be satisfied for materials with a single relaxation mode or narrow relaxation spectrum. We then evaluate the same expressions using asymptotic analysis and direct numerical integration for more representative complex fluids having a wide range of relaxation times and nonlinear responses characterized by damping functions of exponential or Soskey–Winter form. We show that for materials with broad relaxation spectra and sufficiently strong strain-dependent damping the empirical Cox–Merz rule and the Gleissle mirror relations are satisfied either exactly, or to within a constant numerical factor of order unity. By contrast, these relationships are not satisfied in other classes of complex viscoelastic materials that exhibit only weak strain-dependent damping or strain softening.

© 2022 Author(s). All article content, except where otherwise noted, is licensed under a Creative Commons Attribution (CC BY) license (<http://creativecommons.org/licenses/by/4.0/>). <https://doi.org/10.1063/5.0084478>

## I. INTRODUCTION

There are a number of important empirical rules, such as the Cox–Merz rule<sup>1</sup> as well as a second less well-known “forgotten Cox–Merz rule,”<sup>2,3</sup> and the Gleissle mirror relationship,<sup>4</sup> that are often used in linear and non-linear rheology to supplement the available data. These rules have been applied to a wide variety of polymer

melts,<sup>2,5–8</sup> polymer solutions,<sup>5,6,9,10</sup> and hydrogels.<sup>11</sup> Similar principles have been used to develop an extended Cox–Merz rule (or Rutgers–Delaware rule) for suspensions as well as highly filled, yielding, and thixotropic materials.<sup>12–14</sup>

These different empirical rules involve relationships between various measurements of the viscous response in a complex fluid such as the steady shear viscosity, the dynamic viscosity, and the shear stress

growth coefficient measured following the inception of steady shear flow. For many rheologists, including the present authors, the first exposure to these curious empirical relationships is in Chapter 3 of the pioneering text developed by R. Byron Bird with coauthors and former graduate students Armstrong and Hassager.<sup>15</sup> They note that “the Cox–Merz rule has proven very useful in predicting  $\eta(\dot{\gamma})$  when only linear viscoelastic data are available” and show data for a linear polystyrene (PS) melt in which the agreement between  $|\eta^*(\omega)|$  and  $\eta(\dot{\gamma})$  is “within experimental error” at equivalent values of the shear rate and angular frequency. This similarity between the complex viscosity and the steady shear viscosity was first noted by W. P. Cox and E. H. Merz in their 1958 paper in which they show that experimental measurements of the steady shear viscosity  $\eta(\dot{\gamma})$  are a smooth continuation of the complex viscosity  $|\eta^*(\omega)|$  for polystyrene melts.<sup>1</sup> More recently, Snijkers and Vlassopoulos<sup>16</sup> have carefully reviewed the levels of agreement (and disagreement) that can be achieved using the Cox–Merz rule for a range of different complex fluids.

The Cox–Merz rule establishes an approximate equality between the shear rate-dependent steady shear viscosity  $\eta(\dot{\gamma})$  of a complex fluid and the dynamic viscosity at equivalent values of the shear rate and angular frequency,<sup>1</sup> i.e.,

$$\eta(\dot{\gamma}) \cong |\eta^*(\omega)|_{\dot{\gamma}=\omega}. \tag{1}$$

This equality between a non-linear quantity (such as the steady shear viscosity) and a linear viscoelastic property (such as the dynamic viscosity) corresponds to equivalence between two quite distinct material functions when they are evaluated at equal values of the Deborah number ( $De = \omega\tau_c$ ) and Weissenberg number ( $Wi = \dot{\gamma}\tau_c$ ),<sup>17,18</sup> where  $\tau_c$  is some characteristic (or mean) relaxation time of the complex fluid being studied. When viewed from the perspective of a Pipkin diagram<sup>19,20</sup> (in which the flow unsteadiness is represented by the magnitude of the Deborah number along the abscissa and in which a suitable non-linear measure such as the Weissenberg number reports the strength of the flow along the ordinate axis), this relationship is especially surprising, as it represents equivalence between the relevant material functions measured along two completely orthogonal axes!

Several researchers have reported different cases in which constitutive models for complex fluids obey the Cox–Merz rule.<sup>2,3,11</sup> In an early analysis, Booij arrives at a sufficient condition for a viscoelastic material to follow the Cox–Merz rule that is independent of the linear relaxation spectrum.<sup>2</sup> The condition states that the non-linear strain measure (denoted  $S_{12}$  in his work) must satisfy

$$S_{12} = \int_0^{\dot{\gamma}u} J_0(v)dv, \tag{2}$$

where  $J_0$  is the zeroth Bessel function and  $\dot{\gamma}u$  is the accumulated strain in an elapsed time  $u$ . However, he notes that this strain measure oscillates with increasing time and is therefore unphysical; the conditions required to satisfy the Cox–Merz relationship in real fluids thus necessarily involve details of the viscoelastic relaxation spectrum.

It is shown in advanced textbooks (see, for example, Ref. 21) that for models characterized by a single relaxation time such as a simple Maxwell model, when the steady shear viscosity is computed using the Wagner integral constitutive model [which is a special limiting case of the time-strain separable (TSS) Kaye–Bernstein Kearsley Zapas (K-BKZ)

constitutive equation]<sup>22–27</sup> with an exponential damping function, the exponent characterizing the rate-dependence of the steady shear viscosity  $\eta(\dot{\gamma})$  is different from the exponent characterizing the frequency dependence of the dynamic viscosity  $|\eta^*(\omega)|$ . It is thus evident that one needs to consider more complex relaxation functions than a single mode Maxwell model.

In one early study, Larson<sup>28</sup> considers materials with a relaxation modulus of power-law form that follows  $G(t) \simeq St^{-\beta}$ . Again, utilizing the Wagner integral formulation he derives an analytic condition required to satisfy the Cox–Merz rule for two different forms of the damping function [an exponential damping function and the Doi–Edwards (DE) damping function].<sup>28</sup> Complex materials exhibiting a power-law stress relaxation response of this functional form are known as *critical gels*.<sup>29</sup> However, the majority of real complex fluids such as polymer solutions and melts are not critical gels and, also, may not follow the exponential or Doi–Edwards strain damping form. Thus, it is not straightforward to apply the Cox–Merz criterion developed by Larson to our understanding of numerous experimental reports in the literature of materials that closely satisfy the Cox–Merz rule.<sup>1,2,5,7,9–11</sup>

In an early extensive study on polystyrene solutions and melts, Yasuda and coworkers<sup>10</sup> examine the agreement (and disagreement) of their data with the Cox–Merz rule. Recently, Snijkers and Vlassopoulos<sup>16</sup> reviewed data for a large variety of different, well-defined polymers (linear monodisperse and polydisperse polymers, star polymers, model branched polymers with more than one branch point, as well as blends of linear polymers of the same chemistry) and found the Cox–Merz rule to work remarkably well for a large variety of molecular structures of flexible polymers with only minor deviations at high shear rates.

Using general arguments and a general Maxwell–Wiechert model (consisting of multiple discrete relaxation time scales), Renardy argues that for viscoelastic materials with a sufficiently broad relaxation spectrum, the Cox–Merz rule will be followed to within a prefactor.<sup>30</sup> It is thus desirable to consider extensions to the analysis of Larson<sup>28</sup> to other related functional forms of the relaxation spectrum and other types of strain damping function. In the present work, we do this by using an integral formulation of the fractional Maxwell model and considering a generalized form of the strain damping function.

The empirical relations proposed by Cox and Merz relate dynamic measurements of linear viscoelasticity (at low strains) to steady state measurements of the shear viscosity at large (or infinite) strains. Bird *et al.* also describe another “interesting alternative” to the Cox–Merz rule for predicting the steady shear viscosity from dynamic linear viscoelastic data, which they refer to as the *Gleissle Mirror Relation* crediting observations from Gleissle<sup>4</sup> for a high polymer silicone oil. Gleissle<sup>4</sup> related the bounding linear viscoelastic envelope of the shear stress growth coefficient (following inception of steady shear) to the steady shear viscosity as follows:

$$\lim_{\dot{\gamma}_0 \rightarrow 0} \eta^+(t) \cong \eta(\dot{\gamma})|_{\dot{\gamma}=1/t}. \tag{3}$$

Henceforth in this paper, for compactness, we refer to the limiting curve given by the shear stress growth coefficient during start-up of steady shear at  $Wi \ll 1$  [i.e., the left-hand side of Eq. (3)] as the *transient viscosity*  $\eta^+(t) \equiv \sigma^+(t)/\dot{\gamma}_0$ . This expression is known as the mirror relation since a single measurement of the transient start-up viscosity can be reflected using the mapping  $\dot{\gamma} = 1/t$  to estimate the

functional form of the steady shear viscosity over a wide range of shear rates. When viewed in the framework of a Pipkin diagram,<sup>19</sup> this relationship is just as puzzling as Eq. (1) as it again relates measurements made as a function of the elapsed time  $t$  in the linear viscoelastic regime (i.e., in the limit  $\tau_c \dot{\gamma}_0 \ll 1$ ) to measurements of the steady shear viscosity at all shear rates, even well into the non-linear shear-thinning regime. This relation is discussed by Leblans *et al.*<sup>31</sup> for polymer melts and by Jaishankar for Xanthan gum.<sup>11</sup>

Although these empirical rules have been shown to be obeyed for a wide range of complex fluids, there is limited physical understanding or mathematical derivation of these expressions from general constitutive relationships, such as the K-BKZ model, that interrelate the stress and strain tensors for a wide range of complex fluids.<sup>24,32</sup> In this paper, we discuss in detail the conditions required for a general complex fluid to obey the Cox–Merz rule and the Gleissle mirror relationship. To do this, we use the Wagner integral framework, which is a special limiting case of the time-strain separable K-BKZ constitutive equation describing the tensorial stress–strain relationship in a general frame-invariant way. This constitutive equation has been tested extensively and has been demonstrated to describe accurately the steady and transient shear responses of a wide range of complex fluids.<sup>11,15,22,23,33</sup>

To incorporate the non-linearities that arise at large strain amplitudes within the Wagner integral constitutive equation, we use a generalized form of the damping function often known as the Soskey–Winter damping expression.<sup>34</sup> This functional form has been shown to capture the damping or strain-softening of many complex fluids such as polymer melts, polymers, suspensions, magnetorheological fluids as well as polymer blends at large strains.<sup>22,23,28,35–39</sup> To evaluate the Cox–Merz rule and Gleissle mirror relationships embodied in Eqs. (1) and (3), we also need to specify the form of the viscoelastic relaxation kernel. We first illustrate our approach using the simple Maxwell model that describes materials such as wormlike micellar fluids with a single dominant relaxation time scale, and show analytically using the Wagner integral formulation why such materials do not obey the Cox–Merz relation. Then, in order to represent more realistic complex fluids with a broad relaxation spectrum, we use the fractional Maxwell liquid model (FML) to describe the linear relaxation kernel. The FML model has been shown to compactly describe the linear viscoelastic properties of a wide range of complex fluids that have a finite zero shear viscosity such as polymer melts and polymer solutions.<sup>11,40</sup> In the special limit  $\eta_0 \rightarrow \infty$ , the FML model can also be used to describe critical gels and thus reduces to the same relaxation spectrum considered by Larson.<sup>28</sup>

In a recent study, we have used this constitutive formulation to derive analytical expressions for the rate-dependent viscosity in various *weak* and *strong* damping limits.<sup>40</sup> In the present contribution, we use these analytic results, in conjunction with the linear viscoelastic response of the fractional Maxwell liquid, to show that complex fluids undergoing sufficiently strong strain-softening at large strain amplitudes will obey both the Cox–Merz and Gleissle mirror relations to within a numerical constant. By contrast, other highly elastic materials (which are characterized by very weak damping responses) will deviate from both the empirical Cox–Merz and Gliessele mirror rules. Finally, we illustrate these mathematical expressions using experimental measurements with an 8% alginate solution which is well-described by the FML/Wagner integral framework and indeed satisfies the Cox–Merz and mirror relationships very closely.

## II. MATHEMATICAL FORMULATION

The Wagner integral model, which is a special limiting case of the time-strain-separable K-BKZ constitutive equation,<sup>41</sup> gives the relation between the stress and Finger strain tensor as follows:

$$\boldsymbol{\sigma}(t) = \int_{-\infty}^t M(t-t') h(I_1, I_2) [\mathbf{C}^{-1}(t, t') - \mathbf{I}] dt', \quad (4)$$

where  $M(t-t') \equiv \partial G(t-t')/\partial t'$  is known as the memory function and  $G(t)$  is the linear viscoelastic relaxation modulus. The damping function  $h$  describes the survival probability of elastically active network elements after the application of a sudden large deformation.<sup>23,41</sup> Here,  $I_1$  and  $I_2$  are the first and second invariants of the Finger strain tensor ( $\mathbf{C}^{-1}$ ) and  $\mathbf{I}$  is the identity matrix. For shear flows in which  $I_1 = I_2$ , we can simplify Eq. (4) to arrive at the following integral expression for the shear stress  $\sigma(t)$  at time  $t$ :

$$\sigma(t) = - \int_{-\infty}^t M(t-t') h(\gamma) \gamma(t, t') dt', \quad (5)$$

where the minus sign is present in front of the integral since we follow the dynamics of polymeric liquids (DPL)<sup>15</sup> definition for the strain  $\gamma(t, t') = \gamma(t') - \gamma(t)$  as the accumulated strain between an arbitrary time  $t'$  in the past and the present time  $t$ . The damping function  $h(\gamma)$  is given by<sup>11,23,33</sup>

$$h(\gamma_0) = \frac{G(t, \gamma_0)}{G(t)}, \quad (6)$$

where  $G(t, \gamma_0)$  is the strain-dependent relaxation shear modulus and  $G(t)$  is the linear relaxation modulus (which is independent of strain at small strain amplitudes).

For a steady shearing flow at constant shear rate  $\dot{\gamma}$ , the accumulated strain can be written as  $\gamma(t, t') = \dot{\gamma} \times (t' - t) = -\dot{\gamma}u$ . The steady shear viscosity  $\eta(\dot{\gamma})$  for a constant shear rate  $\dot{\gamma}$  can then be derived from Eq. (5) and written using the change of variables  $u = t - t'$  as

$$\frac{\sigma(\dot{\gamma})}{\dot{\gamma}} \equiv \eta(\dot{\gamma}) = \int_0^\infty M(u) h(\dot{\gamma}u) u du. \quad (7)$$

## III. SINGLE MODE RELAXATION MATERIALS

First, we derive the shear rate dependent viscosity for the canonical case of a simple Maxwell relaxation kernel and an exponential damping function as proposed by Rolon-Garrido and Wagner.<sup>23</sup> In differential form, the simple Maxwell element can be pictured as a series arrangement of a single linear (Newtonian) dashpot and a linear Hookean spring as shown in Fig. 1(a). The corresponding memory function for a Maxwell element can be written as<sup>15</sup>

$$M(t) = \frac{\eta_0}{\tau^2} \exp(-t/\tau), \quad (8)$$

where  $\eta_0$  is the zero shear viscosity and  $\tau$  is the (single) relaxation time scale captured by the model. Thus, the steady shear rate-dependent viscosity for a linear Maxwell element combined with an exponential damping function (which is characterized by a critical strain  $\gamma^*$ ) and written in the form  $h(\gamma) = \exp(-\gamma/\gamma^*) \equiv \exp(-\dot{\gamma}u/\gamma^*)$  becomes

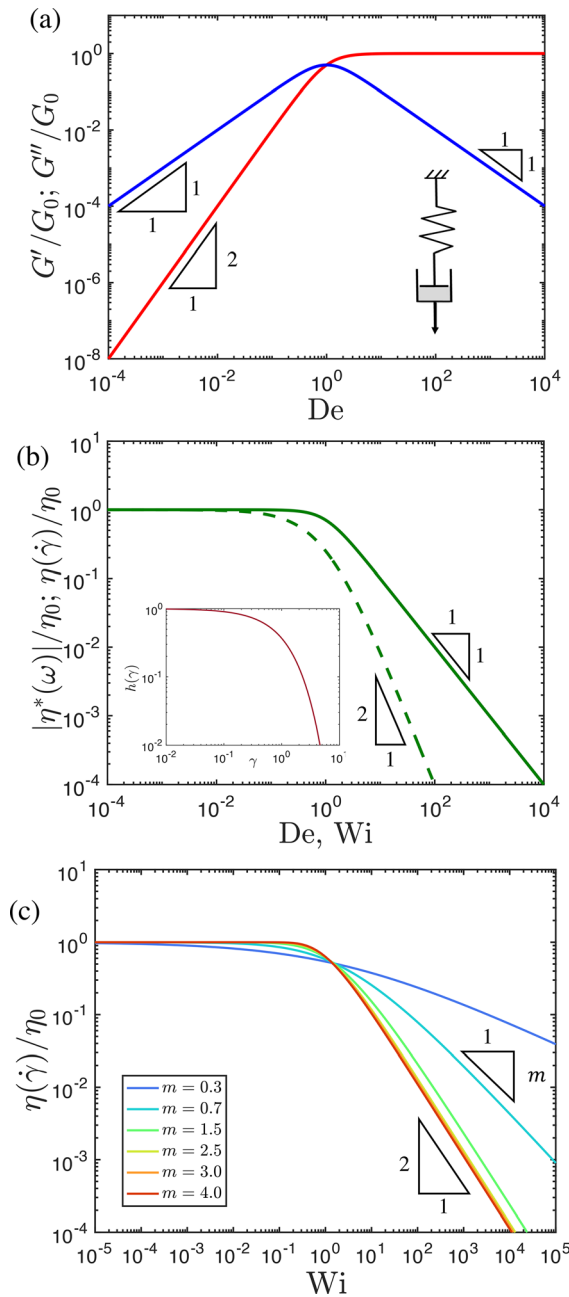


**FIG. 1.** (a) The storage modulus (red solid line) and loss modulus (blue solid line) of the single Maxwell model are represented as functions of the Deborah number  $De = \tau\omega$ . The complex viscosity  $|\eta^*(\omega)|/\eta_0$  and the steady shear viscosity  $\eta(\dot{\gamma})/\eta_0$  evaluated for a single Maxwell kernel with exponential damping are illustrated in (b). The exponential damping function  $h(\gamma)$  with  $\gamma^* = 1$  is shown in the inset. The complex viscosity and the steady shear viscosity progressively deviate as the shear rate increases. (c) The steady shear viscosity for a single mode Maxwell model with generalized damping function given by Eq. (14) for various damping parameters. The asymptotic dependence of the steady shear viscosity at high shear rates for  $m < 2$  is set by the value of damping exponent to be  $\eta \sim \dot{\gamma}^{-m}$ . However, for  $m \geq 2$ , the asymptotic slope of the steady shear viscosity is always  $\eta \sim \dot{\gamma}^{-2}$ , independent of the value of the damping exponent.

$$\eta(\dot{\gamma}) = \int_0^\infty \frac{\eta_0}{\tau^2} \exp(-u/\tau) \exp(-\dot{\gamma}u/\gamma^*) u du. \quad (9)$$

This integral expression for the rate-dependent viscosity can be evaluated analytically and simplified to the form

$$\eta(\dot{\gamma}) = \frac{\eta_0}{(1 + \dot{\gamma}\tau/\gamma^*)^2}. \quad (10)$$

The dimensionless product  $\dot{\gamma}\tau$  can be identified as the Weissenberg number,  $Wi$  measuring the strength of the non-linear shear flow.<sup>17</sup> Thus, Eq. (10) can be written equivalently in dimensionless form as

$$\frac{\eta(\dot{\gamma})}{\eta_0} = \frac{1}{(1 + Wi/\gamma^*)^2}. \quad (11)$$

The magnitude of the complex viscosity  $|\eta^*(\omega)|$  in small amplitude oscillatory shear (SAOS) for the linear Maxwell model is given by<sup>15,40</sup>

$$\frac{|\eta^*(\omega)|}{\eta_0} = \frac{1}{\sqrt{1 + (\omega\tau)^2}}. \quad (12)$$

The product  $\omega\tau$  corresponds physically to the ratio of two time scales ( $\tau$  and the period of oscillation  $T \sim \omega^{-1}$ ) and thus defines the Deborah number ( $De$ ) for this flow. Therefore, the linear complex viscosity can be written as

$$\frac{|\eta^*(\omega)|}{\eta_0} = \frac{1}{\sqrt{1 + (De)^2}}. \quad (13)$$

It is clear from Eqs. (11) and (13) that only at low values of both  $Wi$  and  $De$  is the Cox–Merz rule exactly satisfied for this single relaxation mode model. This corresponds to approaching the origin of a Pipkin diagram<sup>19</sup> and gives the expected simple fluid result

$$\lim_{\dot{\gamma} \rightarrow 0} \eta(\dot{\gamma}) \rightarrow \eta_0 \leftarrow \lim_{\omega \rightarrow 0} |\eta^*(\omega)|.$$

At larger values of the Weissenberg and Deborah numbers, the steady shear viscosity and the complex viscosity deviate systematically from each other. This is illustrated graphically in Fig. 1. At high values of the imposed oscillatory frequency or shear rate (corresponding to  $De \gg 1$  and  $Wi \gg 1$ , respectively), the complex viscosity scales as  $|\eta^*(De \gg 1)| \sim De^{-1}$  and the steady shear viscosity scales as  $\eta(Wi/\gamma^* \gg 1) \sim Wi^{-2}$ .

Next, we consider a more generalized form of the damping function also known as the Soskey–Winter damping function<sup>34</sup>

$$h(\gamma) = \frac{1}{1 + (\gamma/\gamma^*)^m}, \quad (14)$$

where  $\gamma^*$  again corresponds to the critical strain and  $m$  is the damping exponent. The damping function in the Doi–Edwards constitutive equation with independent alignment assumption (DE-IAA) can be approximated by a special case of this general Soskey–Winter damping form<sup>23</sup> with a damping exponent  $m=2$  and a critical strain  $\gamma^* = \sqrt{15}/2$ .

The critical strain parameter  $\gamma^*$  is connected physically to the idea of a maximum in the effective strain imparted to a transient network during a rapid step deformation {i.e.,  $\max[h(\gamma)\gamma]$ }. Beyond this critical strain level, the effective strain imparted to the network starts

decreasing due to strain-softening effects such as chain disentanglement or non-affine deformation. For the exponential damping function used in Eq. (9), as well as the approximate form of the Doi–Edwards damping function ( $m = 2$ ) this occurs exactly at  $\gamma^*$ . For a general Soskey–Winter damping with  $m > 1$  (but  $m \neq 2$ ), the maximum effective strain is still controlled by the critical strain parameter, but is not identically equal to  $\gamma^*$ . For weaker damping with  $m \leq 1$ , the effective strain increases without bound irrespective of the critical strain parameter.

Using this form of the damping function and combining Eqs. (7) and (14), we obtain

$$\eta(\dot{\gamma}) = \int_0^\infty \frac{\eta_0}{\tau^2} \exp(-u/\tau) \frac{1}{1 + (\dot{\gamma}u/\gamma^*)^m} u \, du. \quad (15)$$

This expression can readily be evaluated numerically for any value of the shear rate, but we can also obtain asymptotic expressions for the rate-dependent viscosity at low and high shear rates, respectively. To do this, we approximate the integral Eq. (15) using the limiting forms of the damping function  $h(\gamma)$  at small strains ( $Wi/\gamma^* \ll 1$ ) and at large strains ( $Wi/\gamma^* \gg 1$ ) to obtain

$$\frac{\eta(\dot{\gamma})}{\eta_0} \approx \int_0^{\gamma^*/Wi} v \exp(-v) \, dv + \left(\frac{\gamma^*}{Wi}\right)^m \int_{\gamma^*/Wi}^\infty v^{1-m} \exp(-v) \, dv, \quad (16)$$

where the argument  $v = u/\tau$  is a dimensionless time. At low shear rates, this expression is dominated by the first integral<sup>40</sup> and approaches the zero shear-rate viscosity  $\eta(Wi/\gamma^* \ll 1) = \eta_0$ . Similarly, the asymptote for the rate-dependent viscosity at high shear rates (which is dominated by the second integral) can be found to be<sup>40</sup>

$$\lim_{Wi/\gamma^* \gg 1} \frac{\eta(\dot{\gamma})}{\eta_0} = \left(\frac{\gamma^*}{Wi}\right)^m \Gamma_u\left(2 - m, \frac{\gamma^*}{Wi}\right), \quad (17)$$

where  $\Gamma_u(s, x) = \int_x^\infty t^{s-1} e^{-t} dt$  is the upper incomplete Gamma function. From Eq. (17), it can be shown<sup>42</sup> that for values of the damping exponent  $m < 2$ , we have  $\eta(Wi/\gamma^* \gg 1)/\eta_0 \approx \Gamma(2 - m)(Wi/\gamma^*)^{-m}$ , and for the damping exponents  $m \geq 2$ , the rate-dependent viscosity scales as  $\eta(Wi/\gamma^* \gg 1)/\eta_0 \sim (Wi/\gamma^*)^{-2}$ .

In the linear viscoelastic limit of small strains, strain damping is unimportant and the complex viscosity is again given by Eq. (13). In the limit of high frequencies, it thus always scales as  $|\eta^*(De \gg 1)| \sim De^{-1}$  regardless of the form of the damping function. This deviation between the rate-dependent viscosity and complex viscosity explains why polymeric materials with very narrow relaxation spectra or single dominant relaxation modes generally do not satisfy the Cox–Merz relationship. For completeness, the asymptotic limits of the complex viscosity and steady shear rate-dependent viscosity are tabulated in Table I.<sup>43</sup>

#### IV. MATERIALS WITH BROAD RELAXATION SPECTRA

##### A. Cox–Merz relations for broad relaxation materials

We now extend the above analysis to consider more realistic complex fluids that are typically characterized by broad relaxation spectra. We use the fractional Maxwell liquid model (FML) to describe the linear viscoelastic properties of such materials in a compact way. The constitutive relation for the evolution of the shear stress in the FML model can be written in differential form as

**TABLE I.** The asymptotes of the complex viscosity and the steady shear rate-dependent viscosity for a single mode Maxwell memory kernel [Eq. (8)] and various forms of the damping function. It is clear from this table that at high Deborah numbers ( $\tau\omega \gg 1$ ) and high Weissenberg numbers ( $\tau\dot{\gamma} \gg 1$ ), the Cox–Merz relation is, in general, not satisfied.

	$h(\gamma)$	$ \eta^*(\omega) /\eta_0$	$\eta(\dot{\gamma})/\eta_0$
De, $Wi/\gamma^* \ll 1$	$\exp(-\gamma/\gamma^*)$	$= 1$	$= 1$
	$\frac{1}{1 + (\gamma/\gamma^*)^m} \quad m < 2$	$= 1$	$= 1$
	$\frac{1}{1 + (\gamma/\gamma^*)^m} \quad m \geq 2$	$= 1$	$= 1$
De, $Wi/\gamma^* \gg 1$	$\exp(-\gamma/\gamma^*)$	$\sim De^{-1}$	$\sim \left(\frac{Wi}{\gamma^*}\right)^{-2}$
	$\frac{1}{1 + (\gamma/\gamma^*)^m} \quad m < 2$	$\sim De^{-1}$	$\sim \left(\frac{Wi}{\gamma^*}\right)^{-m}$
	$\frac{1}{1 + (\gamma/\gamma^*)^m} \quad m \geq 2$	$\sim De^{-1}$	$\sim \left(\frac{Wi}{\gamma^*}\right)^{-2}$

$$\sigma(t) + \frac{\eta_0}{\mathbb{G}} \frac{d^{1-\beta} \sigma(t)}{dt^{1-\beta}} = \eta_0 \frac{d\gamma(t)}{dt}. \quad (18)$$

It is necessary for the exponent  $\beta$  to satisfy  $0 \leq \beta \leq 1$  for thermodynamic consistency,<sup>44</sup> and the parameter  $\eta_0$  in Eq. (18) corresponds to the zero shear viscosity of the fluid.<sup>11</sup>

It can be shown that this model is also a compact approximation of the linear viscoelastic response predicted by the Rouse and the Zimm models when  $\beta = 0.5$  and  $\beta = 0.66$ , respectively.<sup>45,46</sup> The parameter  $\mathbb{G}$  in the model is best described as a quasiproperty<sup>47</sup> with units of Pa s <sup>$\beta$</sup> .

The critical gel model studied by Winter and coworkers is also embodied within this constitutive framework. In the limit of infinite zero-shear viscosity ( $\eta_0 \rightarrow \infty$ ), the mean relaxation time in the FML model diverges to infinity  $\tau_c \sim (\eta_0/\mathbb{G})^{1/(1-\beta)} \rightarrow \infty$ , and the effective modulus goes to zero,  $G_e \sim (\eta_0^{-\beta}/\mathbb{G})^{1/(1-\beta)} \rightarrow 0$ . After taking this limit in the differential equation (18) and integration [by a fractional order of  $(1 - \beta)$ ], we obtain the familiar limit of a critical gel,<sup>29</sup> which corresponds to a “Scott Blair element,”<sup>47</sup> i.e., a single spring–pot element with power-law exponent  $\beta$  and a gel strength  $S$  that is related to the quasi-property  $\mathbb{G}$  by  $S = \mathbb{G}/\Gamma(1 - \beta)$ .

Considering a step strain response, we can calculate the relaxation modulus of the FML model from Eq. (18) as<sup>48</sup>

$$\frac{\sigma(t)}{\gamma_0} \equiv G(t) = \mathbb{G} t^{-\beta} E_{1-\beta, 1-\beta} \left( -\frac{\mathbb{G}}{\eta_0} t^{1-\beta} \right), \quad (19)$$

where  $E_{a,b}(x)$  is the Mittag–Leffler function.<sup>49</sup> The characteristic time scale for the three-parameter FML model is given by:  $\tau_c = (\eta_0/\mathbb{G})^{1/(1-\beta)}$  and this allows the argument of the Mittag–Leffler function to be compactly written in terms of a dimensionless time  $t/\tau_c$ . From here, the memory function can be found from the expression  $M(t) \equiv -\partial G(t)/\partial t$ . Thus,

$$M(t) = -\eta_0 (t/\tau_c)^{1-\beta} E_{1-\beta, -\beta} \left( -(t/\tau_c)^{1-\beta} \right), \quad (20)$$

where the negative sign appears from the differentiation (in time) of the (monotonically decreasing) relaxation modulus.

The fractional differential operator in Eq. (18) is nonlocal in time and captures a broadly distributed response to an imposed deformation. The viscoelastic response described by a fractional differential constitutive equation can also be equivalently represented in terms of a continuous relaxation spectrum,  $H(\tau)$ , which quantifies the contribution of different relaxation time scales  $\tau$  to the viscoelastic memory exhibited by a hereditary material.<sup>50,51</sup> To see this, we note that the relaxation modulus can be written in terms of the relaxation spectrum as<sup>15</sup>

$$G(t) = \int_{-\infty}^{\infty} \exp(-t/\tau) H(\tau) d \ln \tau. \quad (21)$$

Combining this result and the relaxation modulus given in Eq. (19), a Stieltjes transform<sup>52</sup> can be used to obtain

$$\frac{H_0(\tau)}{\eta_0/\tau_c} = \frac{1}{\pi} \frac{(\tau/\tau_c)^{-1} \sin(\pi\beta)}{(\tau/\tau_c)^{\beta-1} + (\tau/\tau_c)^{1-\beta} - 2 \cos(\pi\beta)}. \quad (22)$$

This is a special limit of the more general result that can be derived for the full fractional Maxwell model<sup>53,54</sup> when  $\alpha = 1$ . The evolution in the shape of the relaxation spectrum for the FML model for different values of  $\beta$  is shown in Fig. 2 and illustrates the compactness of using a fractional model to describe broad relaxation spectra. The relaxation spectra shown in Fig. 2 for the values of  $\beta = 0.5$  and  $\beta = 0.66$  closely approximate the Rouse and Zimm relaxation spectra, respectively.<sup>45</sup> As the value of  $\beta$  approaches zero, the relaxation spectrum becomes narrower and eventually approaches a singular (delta) function for  $\beta = 0$  which corresponds to the simple Maxwell model limit described in Sec. III.

The dynamic modulus  $G^*(\omega)$  of the FML model can be obtained by taking a Fourier transform of the linear differential equation in time represented by Eq. (18) and is given by

$$G^*(\omega) = \frac{G(i\omega)^\beta \cdot \eta_0(i\omega)}{G(i\omega)^\beta + \eta_0(i\omega)}. \quad (23)$$

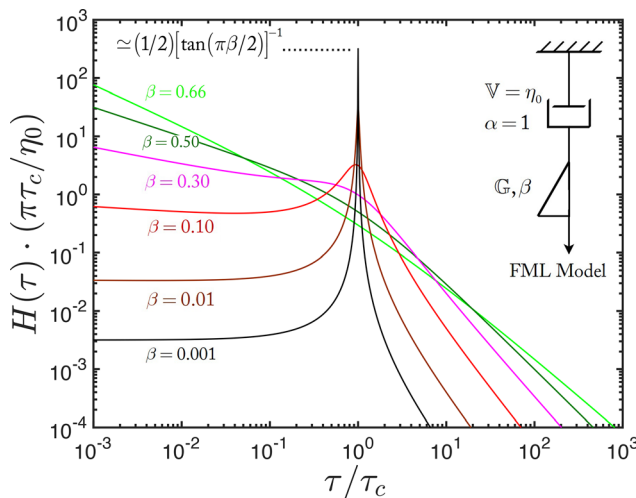


**FIG. 2.** Evolution of the continuous relaxation spectrum  $H(\tau)$  corresponding to the fractional Maxwell liquid (FML) as the exponent  $\beta$  is changed, while the viscosity  $\eta_0$  and characteristic time constant  $\tau_c$  are held constant. In the limit  $\beta \rightarrow 0$ , the relaxation spectrum approaches a delta function response corresponding to a single mode Maxwell model.

The real and imaginary parts of the complex modulus can be found from Eq. (23) and hence the expressions for the storage and loss modulus of the FML model can be written as follows:

$$\frac{G'(\omega)}{G_c} = \frac{(\omega\tau_c) \cos(\pi/2) + (\omega\tau_c)^{2-\beta} \cos(\pi\beta/2)}{1 + (\omega\tau_c)^{1-\beta} \cos(\pi(1-\beta)/2) + (\omega\tau_c)^{2(1-\beta)}}, \quad (24)$$

$$\frac{G''(\omega)}{G_c} = \frac{(\omega\tau_c) \sin(\pi/2) + (\omega\tau_c)^{2-\beta} \sin(\pi\beta/2)}{1 + (\omega\tau_c)^{1-\beta} \cos(\pi(1-\beta)/2) + (\omega\tau_c)^{2(1-\beta)}}, \quad (25)$$

where  $G_c = \eta_0\tau_c^{-1} = G\tau_c^{-\beta}$  is the characteristic elastic modulus of the FML model, and the Deborah number can again be identified as  $De = \tau_c\omega$ .

The magnitude of the complex viscosity, defined as  $|\eta^*(\omega)| = \sqrt{G'(\omega)^2 + G''(\omega)^2}/\omega$ , can then be evaluated from Eqs. (24) and (25) and expressed in compact dimensionless form as

$$\frac{|\eta^*(\omega)|}{\eta_0} = \frac{1}{\sqrt{1 + 2(De)^{1-\beta} \cos(\pi(1-\beta)/2) + (De)^{2-2\beta}}}. \quad (26)$$

The low and high Deborah number asymptotes for the complex viscosity can be calculated from Eq. (26) to be

$$\lim_{De \ll 1} \frac{|\eta^*(\omega)|}{\eta_0} = 1 \quad (27)$$

and

$$\lim_{De \gg 1} \frac{|\eta^*(\omega)|}{\eta_0} = De^{-(1-\beta)}. \quad (28)$$

In all of the above expressions, the simple linear Maxwell model corresponding to a single spring and dashpot can be retrieved by substituting  $\beta = 0$  in Eqs. (18)–(27). This would lead us to a single dominant relaxation time scale as illustrated in Fig. 2 characterized by a single dominating microstructural length scale. As shown in Sec. III, this would lead to failure of the Cox–Merz rule and Gleissle mirror relation irrespective of the damping function.

The rate-dependent viscosity defined in Eq. (7) evaluated with a linear FML kernel specified by Eq. (20) can then be written quite generally as

$$\frac{\eta(\dot{\gamma})}{\eta_0} = -\tau_c^{\beta-1} \int_0^\infty u^{-\beta} E_{1-\beta, -\beta} \left( -(u/\tau_c)^{1-\beta} \right) h(\dot{\gamma}u) du. \quad (29)$$

In our earlier work,<sup>40</sup> we derived an approximate analytical expression for the above integral using the exponential damping function  $h(\gamma) = \exp(-\gamma/\gamma^*)$ , which can be written in terms of a two-part summation as follows:

$$\begin{aligned} \frac{\eta(\dot{\gamma})}{\eta_0} = & \mathcal{H} \left( 1 - \frac{Wi}{\gamma^*} \right) \sum_{k=1}^{\infty} (-1)^{k+1} (\beta + k(1-\beta)) \left( \frac{Wi}{\gamma^*} \right)^{(k-1)(1-\beta)} \\ & + \mathcal{H} \left( \frac{Wi}{\gamma^*} - 1 \right) \left( \frac{Wi}{\gamma^*} \right)^{\beta-1} \sum_{k=1}^{\infty} (-1)^{k+1} (1 - k(1-\beta)) \\ & \times \left( \frac{Wi}{\gamma^*} \right)^{-(k-1)(1-\beta)}, \end{aligned} \quad (30)$$

where  $\mathcal{H}$  is the Heaviside step function. In Ref. 40, we denoted exponential damping as a *strong* damping function since the exponent describing the rate-dependence of the viscosity at high shear rates is

set by the FML linear kernel parameter [i.e.,  $\eta \sim \dot{\gamma}^{-(1-\beta)}$ ] and not by the parameters of the damping function itself.

The low Weissenberg number asymptote for the steady shear viscosity can be obtained from the first term in Eq. (30) above and reduces to

$$\lim_{Wi/\gamma^* \ll 1} \frac{\eta(\dot{\gamma})}{\eta_0} = 1, \quad (31)$$

whereas the high Wi asymptote is given by

$$\lim_{Wi/\gamma^* \gg 1} \frac{\eta(\dot{\gamma})}{\eta_0} = \beta \left( \frac{Wi}{\gamma^*} \right)^{\beta-1}. \quad (32)$$

By comparing Eqs. (27) and (31), it is easy to note that the steady and complex viscosity converge to the same value, corresponding to the zero shear rate viscosity  $\eta_0$  at low Wi or De, as expected for a “simple fluid.”<sup>55</sup> By comparing Eqs. (28) and (32), we observe that the power-law exponents describing the dependence on De and Wi are also equal and therefore the Cox–Merz relation is always satisfied (to within a constant numerical prefactor) for the integral constitutive equation given by Eq. (5) with an FML kernel and an exponential strain-dependent function.

We can also arrive at a condition to *identically* satisfy the Cox–Merz relation, i.e.,  $\eta(\dot{\gamma}) = |\eta^*(\omega)|$  at high Wi or De by equating Eqs. (28) and (32). We thus obtain the constraint

$$\gamma^* = \beta^{\frac{1}{\beta-1}}. \quad (33)$$

This expression provides a relationship between the critical strain parameter  $\gamma^*$  and the FML exponent  $\beta$  needed to identically satisfy the Cox–Merz relation. If we consider the Rouse model in which the high frequency linear viscoelastic response is set by  $G' \sim \omega^{0.5}$ , then we find  $\gamma^*_{(R)} = (0.5)^{1/(0.5-1)} = 4$ . Similarly, if we consider the Zimm model with  $\beta = 0.66$  we obtain  $\gamma^*_{(Z)} = (0.66)^{1/(0.66-1)} = 3.4$ . It is typical for entangled polymer solutions and melts to have  $\gamma^* = 1 \leq \gamma^* \leq 4$  (Ref. 15) (see also the Appendix). It is apparent that the Cox–Merz relationship will therefore always be very closely approximated [especially given the form of Eq. (33) and the fact that we graphically represent viscometric measurements on double logarithmic axes].

We can also consider the rate-dependent viscosity for the more general damping function of  $h(\gamma) = [1 + (\gamma/\gamma^*)^m]^{-1}$  by evaluating Eq. (29) and then obtain<sup>40</sup>

$$\begin{aligned} \frac{\eta(\dot{\gamma})}{\eta_0} &= \mathcal{H}(1 - Wi/\gamma^*) \\ &\times \sum_{k=1}^{\infty} \left[ \frac{(-1)^{k+1} p \pi}{m \Gamma(1-p) \sin\left(\pi \frac{(1-p)}{m}\right)} \left(\frac{Wi}{\gamma^*}\right)^{(k-1)(1-\beta)} \right] \\ &+ \mathcal{H}(Wi/\gamma^* - 1) \left(\frac{Wi}{\gamma^*}\right)^{\beta-1} \\ &\times \sum_{k=1}^{\infty} \left[ \frac{(-1)^{k+1} q \pi}{m \Gamma(1-q) \sin\left(\pi \frac{(1-q)}{m}\right)} \left(\frac{Wi}{\gamma^*}\right)^{-(k-1)(1-\beta)} \right], \end{aligned} \quad (34)$$

where  $p = \beta + k(1 - \beta)$ ,  $q = 1 - k(1 - \beta)$ . The asymptotes of this expression are dominated by the  $k=1$  terms. The low Weissenberg number asymptote can be calculated from the first term in Eq. (34) to once again be

$$\lim_{Wi/\gamma^* \ll 1} \frac{\eta(\dot{\gamma})}{\eta_0} = 1. \quad (35)$$

However, care must be taken in evaluating the viscosity at high Weissenberg numbers as we have shown<sup>40</sup> that the high Wi limit of Eq. (34) is valid only when  $m > 1 - \beta$ . The two different limiting cases are shown in Figs. 3(a) and 3(b), respectively.

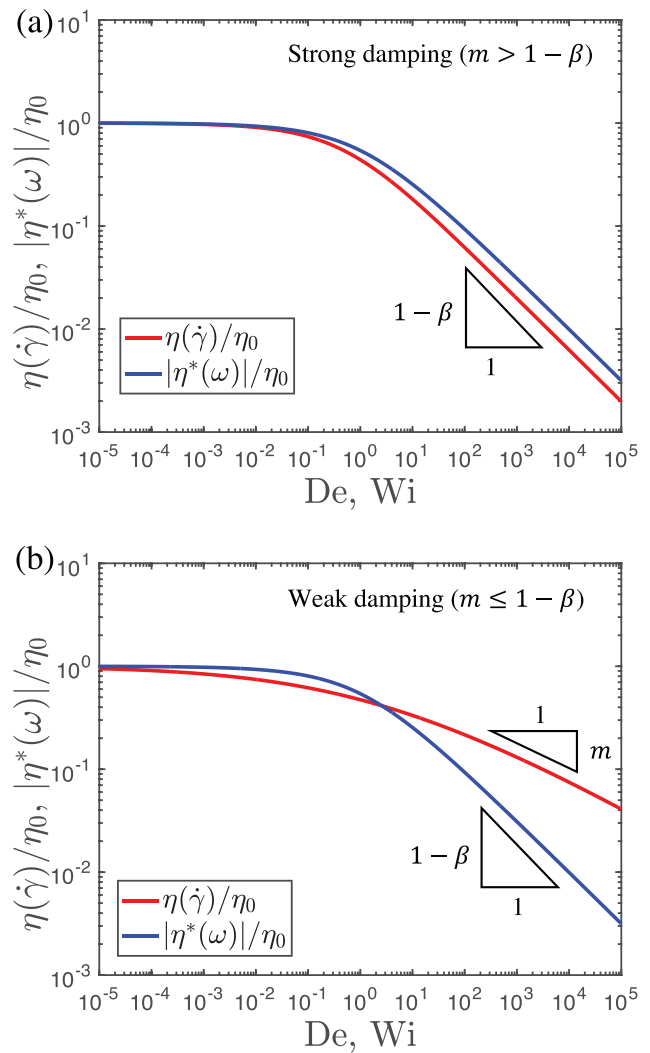


**FIG. 3.** Comparison of the complex viscosity and the rate-dependent viscosity for a damping function of Soskey–Winter form in the limit of (a) strong damping functional forms ( $m > 1 - \beta$ ) and (b) weak damping. For strong damping functions, the Cox–Merz relation is satisfied to within a constant multiplicative factor. However, the Cox–Merz relation fails for weak strain-dependent functional forms  $m \leq (1 - \beta)$ . Here, the model values in panel (a) are  $\beta = 0.5$ ,  $\gamma^* = 1$ , and  $m = 2$  and the model values in panel (b) are  $\beta = 0.5$ ,  $\gamma^* = 1$ , and  $m = 0.3$ .



Provided that we satisfy the constraint  $m > 1 - \beta$ , the asymptotic expression for the rate-dependent viscosity given by Eq. (34) is

$$\lim_{Wi/\gamma^* \gg 1} \frac{\eta(\dot{\gamma})}{\eta_0} = \frac{\pi\beta}{m\Gamma(1-\beta)\sin\left[\frac{\pi(1-\beta)}{m}\right]} \left(\frac{Wi}{\gamma^*}\right)^{\beta-1}. \quad (36)$$

The exponent of the rate-dependent viscosity at high  $Wi$  is thus  $\eta(\dot{\gamma}) \sim \dot{\gamma}^{-(1-\beta)}$ . In Ref. 40, we derived a uniformly valid expression for the steady shear viscosity for the case  $m > 1 - \beta$  that accurately approximates the rate-dependent viscosity for all  $Wi$  and that can be compactly written in the form

$$\frac{\eta}{\eta_0} = \frac{1}{1 + (1/B)(Wi/\gamma^*)^{(1-\beta)}}, \quad (37)$$

where the constant  $B$  is given by

$$B = \frac{\pi\beta}{m\Gamma(1-\beta)\sin\left[\pi\left(\frac{1-\beta}{m}\right)\right]}. \quad (38)$$

This general functional form is similar to several common empirical expressions, such as the Carreau–Yasuda model and Cross model,<sup>10,15,56,57</sup> which are used in the rheology literature for fitting experimentally measured flow curves of  $\eta(\dot{\gamma})$ .

However, for the case  $m \leq 1 - \beta$ , Eq. (34) is invalid and in our previous paper<sup>40</sup> we have derived an alternative expression for the rate-dependent viscosity in the high  $Wi$  limit:

$$\lim_{Wi/\gamma^* \gg 1} \frac{\eta(\dot{\gamma})}{\eta_0} = f(m) \left(\frac{Wi}{\gamma^*}\right)^{-m}, \quad (39)$$

where

$$f(m) = \int_0^\infty -x^{-\beta-m} E_{1-\beta, -\beta}(-x^{1-\beta}) dx. \quad (40)$$

For the case  $m \leq 1 - \beta$ , the exponent describing the rate-dependence of the viscosity is therefore  $\eta(\dot{\gamma}) \sim \dot{\gamma}^{-m}$  as shown in Fig. 3(b). We refer to damping functional forms in which the slope of the rate-dependent viscosity at high  $Wi$  is set by the linear viscoelastic parameter  $(1 - \beta)$  as the *strong* damping limit. For the general Soskey–Winter functional form of Eq. (14), the strong damping condition is therefore  $m > 1 - \beta$ . Cases in which the high  $Wi$  slope is set by the damping parameter  $m$  itself correspond to *weak damping* and in the Soskey–Winter framework correspond to  $m \leq (1 - \beta)$ . As we noted above, the damping function in the Doi–Edwards constitutive equation with the independent alignment assumption (DE-IAA) is of the form given by Eq. (14) with a damping exponent  $m = 2$  and a critical strain  $\gamma^* = \sqrt{15}/2 = 1.94$ .<sup>23</sup> Since the damping exponent  $m = 2$  is always greater than the linear FML parameter  $1 - \beta$  (for  $0 \leq \beta < 1$ ), the damping function from the DE model with independent alignment is thus always of strong damping character.

By comparing Eq. (27) with Eq. (35), we notice that for viscoelastic liquids the Cox–Merz relation is always satisfied at low shear rates and frequencies, or more formally, as the dimensionless values of  $Wi/\gamma^*$  and  $De$  approach zero. By comparing Eq. (28) with Eqs. (36)

and (39), we notice that the Cox–Merz rule is satisfied to within a multiplicative constant factor for strong damping functions, but will not hold at high shear rates or frequencies for functional forms corresponding to weak damping. Again for completeness, the asymptotes for the complex and rate-dependent viscosity for the different damping functional forms are tabulated in Table II.

For the general Soskey–Winter damping expression, we can also determine when the Cox–Merz relationship is identically satisfied by equating the asymptotic expression for the rate-dependent viscosity at high Weissenberg numbers with the frequency-dependent complex viscosity at high Deborah numbers. Setting Eqs. (28) and (36) to be equal, we obtain the dimensionless constraint

$$\frac{\pi\beta(\gamma^*)^{1-\beta}}{m\Gamma(1-\beta)\sin\left[\frac{\pi(1-\beta)}{m}\right]} = 1. \quad (41)$$

This constraint represents a condition interrelating three of the constitutive parameters of a fractional Maxwell/Wagner liquid: the critical strain  $\gamma^*$ , the damping exponent  $m$ , and the linear exponent  $\beta$  (characterizing the short time power-law decay of the relaxation modulus and the power-law dependence of the complex modulus at high frequencies).

Numerical calculations show that even when Eq. (41) is satisfied, there can still be some deviation from the Cox–Merz relation when  $Wi \sim 1$  and  $De \sim 1$ . To illustrate this, we highlight in Fig. 4(a) the deviations between the complex viscosity and the steady shear viscosity. This is reported in terms of the logarithm of the ratio  $|\eta^*(\omega)|/\eta(\dot{\gamma})$  [i.e., we plot contours of  $\log(|\eta^*(\omega)|/\eta(\dot{\gamma}))$ ] for a range of different damping exponents  $m$  and for equal values of  $De$  and  $Wi$ . Exact correspondence with the Cox–Merz rule corresponds to a contour value of

**TABLE II.** Asymptotes of the complex viscosity and steady shear rate-dependent viscosity for the fractional Maxwell liquid kernel for various damping functions. It is clear from this table that when  $De = Wi$ , the Cox–Merz relation is not satisfied for weak damping functions  $m < (1 - \beta)$  but is satisfied to within a numerical constant for strong damping functions corresponding to the exponential form or the Soskey–Winter form with  $m \geq (1 - \beta)$ .

	$h(\gamma)$	$ \eta^*(\omega) /\eta_0$	$\eta(\dot{\gamma})/\eta_0$
$De, Wi/\gamma^* \ll 1$	$\exp(-\gamma/\gamma^*)$	$= 1$	$= 1$
	$\frac{1}{1 + (\gamma/\gamma^*)^m}$	$= 1$	$= 1$
	$m > (1 - \beta)$	$= 1$	$= 1$
$De, Wi/\gamma^* \gg 1$	$\exp(-\gamma/\gamma^*)$	$\sim De^{-(1-\beta)}$	$\sim \left(\frac{Wi}{\gamma^*}\right)^{-(1-\beta)}$
	$\frac{1}{1 + (\gamma/\gamma^*)^m}$	$\sim De^{-(1-\beta)}$	$\sim \left(\frac{Wi}{\gamma^*}\right)^{-(1-\beta)}$
	$m \geq (1 - \beta)$	$\sim De^{-(1-\beta)}$	$\sim \left(\frac{Wi}{\gamma^*}\right)^{-m}$

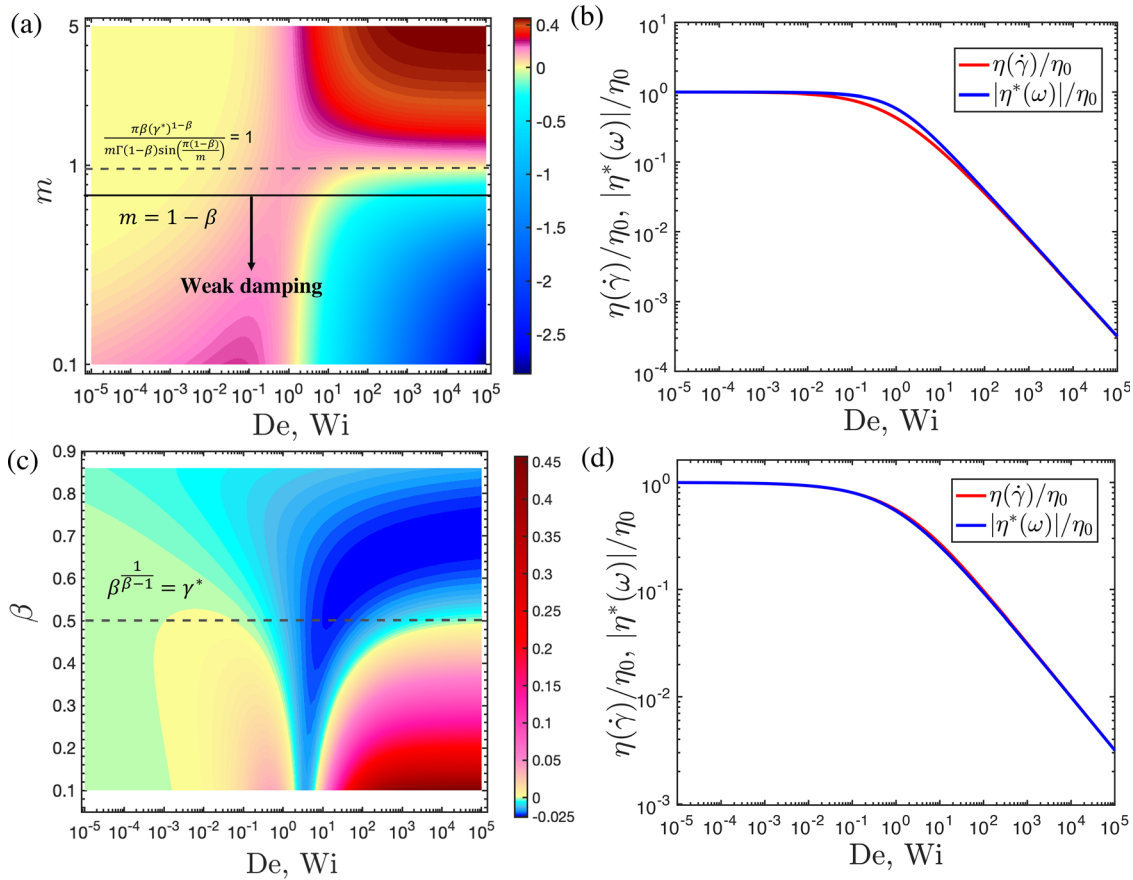


**FIG. 4.** (a) Contour plot of the difference between the logarithm of complex and steady shear viscosity [i.e.,  $\log(|\eta^*(\omega)|/\eta(\dot{\gamma}))$ ] to illustrate the deviation from the Cox–Merz relation for the FML model with a generalized damping function of Soskey–Winter form [Eq. (14)] for various damping exponents  $m$  and De or Wi using an FML parameter of  $\beta = 0.3$  and a critical strain  $\gamma^* = 1$ . The black solid line serves as the demarcation between the regions of weak and strong damping functions. The Cox–Merz relationship is never satisfied for weak damping forms at high Wi resulting in potentially large errors. The gray dashed line represents the result in Eq. (41) when the error is minimum and approaches zero at both low and high Wi. (b) Comparison between the complex and steady shear viscosity when Eq. (41) is followed, showing close agreement with the Cox–Merz relationship. (c) Error contour plot showing the difference  $\log(|\eta^*(\omega)|/\eta(\dot{\gamma}))$  for the FML linear relaxation modulus with an exponential damping  $h(\gamma) = \exp(-\gamma/\gamma^*)$  for a critical strain  $\gamma^* = 4$ . The gray dashed line represents Eq. (33) when the error approaches zero across the full range of deformation rates. (d) The complex viscosity and steady shear viscosity computed using an exponential damping function overlap on top of each other when  $Wi = De$ , showing perfect agreement with the Cox–Merz rule when Eq. (33) is obeyed.

$\log(1) = 0$  and yellow-colored regions of the contour plot. At low deformation rates, the error is very small for all values of  $m$ . By contrast, at high De and Wi the errors are only small in the *strong* damping limit above the solid black line. The error is minimal and approaches zero for all deformation rates when  $m$  is in the vicinity of the value given by Eq. (41) as shown by the broken gray line. When the ratio  $|\eta^*(\omega)|/\eta(\dot{\gamma})$  is greater than unity, the logarithm is positive and the complex viscosity is therefore *greater* than the steady shear viscosity. At high Wi or De, we can observe this in Fig. 4(a) for values of  $m \geq 1$ , and this corresponds to most experimental observations.<sup>16</sup> However, it is also possible for the ratio to be smaller than unity and the logarithm of the ratio is then negative at high Wi as is visible in Fig. 4(a) for smaller values of the damping exponent  $0.8 \leq m \leq 1$ . This case has also been observed in the literature for highly branched polymer systems.<sup>16</sup> In Fig. 4(b), we show a comparison between the complex viscosity and the steady shear viscosity when the damping

exponent  $m$ , the FML parameter  $\beta$ , and the critical strain  $\gamma^*$  are exactly interrelated by the constraint of Eq. (41). The deviation observed at  $De \simeq Wi \simeq 1$  is only of maximum magnitude 0.17 (corresponding to a ratio of viscosities of approximately 1.5). This close agreement of the Cox–Merz relationship at high and low De or Wi (but with small deviations at intermediate shear rates) is consistent with measurements for worm-like micelles and the non-linear differential viscoelastic model proposed by Manero and coworkers.<sup>58</sup>

A similar error contour plot showing  $\log(|\eta^*(\omega)|/\eta(\dot{\gamma}))$  is illustrated for the exponential damping function with various values of the FML parameter  $\beta$  and at equal values of Deborah and Weissenberg numbers in Fig. 4(c). At high Wi or De, once again the ratio of the dynamic viscosity to the steady shear viscosity may be bigger or smaller than unity. From Fig. 4(c), we observe the steady shear viscosity to be less than the dynamic viscosity for smaller values of  $\beta$  and vice versa at larger values of  $\beta$  at high Wi or De. For values of  $\beta \geq 0.5$ ,

the difference between the two material functions is very small and is minimized when the critical strain  $\gamma^*$  follows Eq. (33). A direct comparison of the complex viscosity and the steady shear viscosity when a complex liquid exhibits exponential damping with the critical strain  $\gamma^*$  and the FML parameter  $\beta$  interrelated by Eq. (33) is shown in Fig. 4(d). It is clear that the Cox–Merz rule is satisfied almost exactly at all deformation rates.

## B. Representative experimental example

To help illustrate the broad applicability of this analysis and the Wagner model with a fractional Maxwell kernel, we consider experimental data obtained with an 8% alginate solution in Fig. 5. This semi-flexible biopolymer can be used to produce biocompatible gel-like materials and the rheology can be varied systematically by changing the alginate concentration and the concentration of divalent crosslinks.<sup>59,60</sup> In order to evaluate the strain-dependent damping function

$h(\gamma)$  for this fluid, we first measure the strain-dependent relaxation modulus  $G(t, \gamma_0)$  as shown in Fig. 5(a) for step strains in the range of  $0.3 \leq \gamma_0 \leq 10$ . A broad power-law decay in the relaxation modulus with time is observed for all imposed strain amplitudes. At small strains ( $\gamma_0 \leq 0.7$ ), the measured relaxation curves superpose—indicating the linear viscoelastic limit. At higher applied strain amplitudes, the measurements of the relaxation modulus are systematically lower. We then shift the strain-dependent relaxation modulus on to the linear relaxation modulus [here taken to be  $G(t, \gamma_0 = 0.3)$ ] to determine the damping values  $h(\gamma) = G(t, \gamma_0)/G(t)$ . The collapsed master curve of the relaxation modulus and the corresponding values of the damping function are plotted in Fig. 5(b). The generalized damping function given by Eq. (14) is regressed to the damping values and the resulting best fit parameters (shown by the solid line) are found to correspond to a critical strain  $\gamma^* = 2.5$  and a damping exponent  $m = 1.4$  (which is significantly smaller than the Doi–Edwards limit,  $m^{DE} = 2$ ). The storage

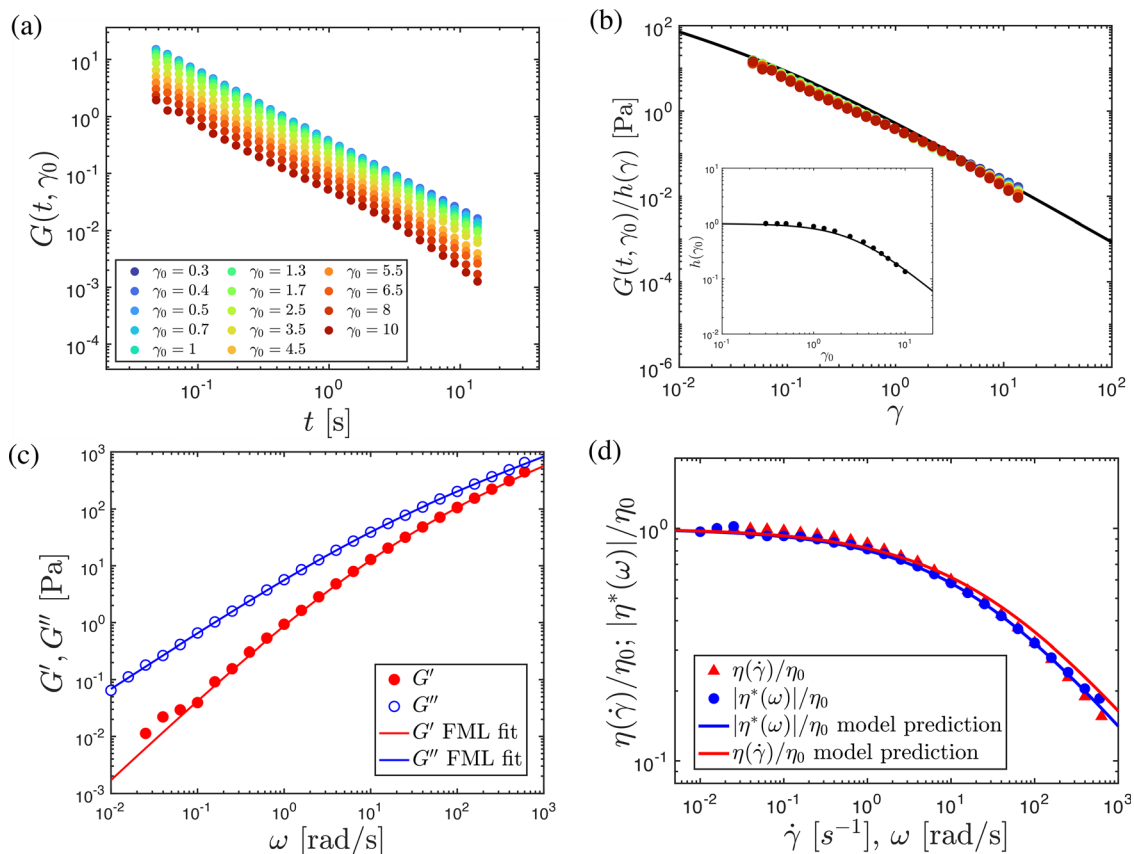


**FIG. 5.** (a) Strain-dependent relaxation modulus for 8% alginate solution for strains up to 1000% ( $\gamma_0 = 10$ ). (b) Superposition of the strain-dependent relaxation modulus to the linear viscoelastic relaxation modulus ( $\gamma_0 \leq 0.7$ ). The solid line indicates the FML fit using the parameters  $G = 23 \text{ Pa s}^\beta$ ,  $\beta = 0.56$ , and  $\eta_0 = 7.0 \text{ Pa s}$ . The damping values are shown in the inset and a damping function of the form of Eq. (14) is used to fit the damping values with parameter values  $\gamma^* = 2.5$  and  $m = 1.4$ . (c) Measurements of the storage modulus (filled) and loss modulus (hollow) at a strain amplitude  $\gamma_0 = 0.02$  are shown and the corresponding FML fit is shown using the same parameter values ( $G = 23 \text{ Pa s}^\beta$ ,  $\beta = 0.56$ , and  $\eta_0 = 7.0 \text{ Pa s}$ ) by the solid lines. (d) Experimental measurements of the steady shear viscosity and magnitude of the complex viscosity evaluated are shown by the data points. The solid lines represent the model predictions from Eq. (26) for the complex viscosity and from Eq. (29) for the steady shear viscosity using the Wagner integral framework with the linear FML kernel and generalized damping function plus the same parameter values given above. The small deviation between the steady shear prediction and the measured data at high shear rates ( $\dot{\gamma} \geq 20 \text{ s}^{-1}$ ) is probably due to experimental artifacts such as partial wall slip or the onset of viscous heating that can become important at high deformation rates.

and loss modulus are obtained by performing SAOS tests for a range of frequencies at a strain amplitude  $\gamma_0 = 0.02$  and are shown in Fig. 5(c). The linear viscoelastic properties of this alginate solution are very well described by the three-parameter fractional Maxwell liquid model as shown in Figs. 5(b) and 5(c), respectively. By regressing the data to Eq. (19), (24), and (25), the best-fit FML parameters are evaluated to be  $G = 23 \text{ Pa s}^\beta$ ,  $\beta = 0.56$ , and  $\eta_0 = 7.0 \text{ Pa s}$ . The characteristic relaxation time is thus  $\tau_c = (7/23)^{1/(1-0.56)} = 0.067 \text{ s}$  and this value can be detected visually by the change in the slope of the storage and loss modulus curves at frequencies around  $\omega_c = 1/\tau_c \simeq 15 \text{ rad/s}$ .

The material properties for this alginate solution thus correspond to the strong damping limit with  $m > (1 - \beta)$  and we should expect the Cox–Merz relationship to be valid. The resulting predictions for the complex viscosity  $|\eta^*(\omega)|$  and the steady shear viscosity  $\eta(\dot{\gamma})$  are illustrated in Fig. 5(d). The FML predictions from Eq. (26) and the prediction for the steady shear viscosity computed from Eq. (29) (with no adjustable parameters) are also compared with the experimental data in Fig. 5(d). The agreement between the measured steady shear data and the Cox–Merz predictions is excellent. The consistency between the experimental data and our chosen time-strain separable (TSS) integral K-BKZ formulation provides validation to the fractional constitutive framework through which we have derived the conditions for the Cox–Merz rule to be satisfied.

### C. The Gleissle mirror relationship

The Gleissle mirror relation relates the time-dependent growth of the transient viscosity at a very low and constant shear rate (i.e., in the linear viscoelastic limit  $\dot{\gamma}_0 \tau_c \ll 1$ ) to the rate-dependent steady shear viscosity<sup>4,61</sup> and can be written in the form

$$\eta^+(t, \dot{\gamma}_0 \rightarrow 0) = \eta(\dot{\gamma} = 1/t). \tag{42}$$

Using the results above, we can determine the conditions required for the Wagner integral constitutive equation with the FML kernel and a generalized damping function to satisfy this empirical relationship. In order for the Gleissle mirror relation to hold true exactly, we find that the following implicit condition must be satisfied between the two parameters characterizing the general damping function ( $\gamma^*$  and  $m$ ) and the parameter  $\beta$  in the FML relaxation kernel:

$$\frac{\pi\beta(\gamma^*)^{1-\beta}}{m\Gamma(1-\beta)\sin\left[\frac{\pi(1-\beta)}{m}\right]} = \frac{\beta}{\Gamma(2-\beta)}. \tag{43}$$

**Derivation of Eq. (43):** The transient viscosity at very low shear rates (in the linear viscoelastic limit) can be found from the integral expression

$$\eta^+(t) \equiv \lim_{\dot{\gamma}_0 \tau_c \ll 1} \eta^+(t, \dot{\gamma}_0) = \int_0^t M(u)u \, du. \tag{44}$$

Substituting the form of the memory function given in Eq. (20) for the FML model into Eq. (44), we obtain

$$\frac{\eta^+(t)}{\eta_0} = -\tau_c^{\beta-1} \int_0^t u^{-\beta} E_{1-\beta, -\beta} \left( -(u/\tau_c)^{1-\beta} \right) du. \tag{45}$$

At early times, during start-up of a steady shear flow, i.e., when  $u/\tau_c \leq t/\tau_c \ll 1$ , the Mittag–Leffler function can be approximated<sup>62</sup> and the above integral reduces to

$$\lim_{t/\tau_c \ll 1} \frac{\eta^+(t)}{\eta_0} = \frac{\beta}{\Gamma(2-\beta)} \left( \frac{t}{\tau_c} \right)^{1-\beta}. \tag{46}$$

At long times  $t/\tau_c \gg 1$ , the steady state shear viscosity in the limit of zero shear rate is

$$\lim_{t/\tau_c \rightarrow \infty} \eta^+(t) = \int_0^\infty M(u)du = \eta_0. \tag{47}$$

From Eqs. (31), (35), and (47), we clearly observe that at long times  $t/\tau_c \gg 1$  both the transient viscosity  $\eta^+(t)$  and the steady-state rate-dependent shear viscosity at an equivalent shear rate  $\eta(\dot{\gamma} = 1/t)$  approach the steady shear viscosity in the limit of zero shear rate,  $\eta_0$ .

If we assume an exponential damping function, then using the Gleissle mirror relationship, the steady shear viscosity at high Wi can be rewritten using Eq. (32) and substituting  $\dot{\gamma} = 1/t$ ; we obtain

$$\lim_{Wi/\gamma^* \gg 1} \frac{\eta(\dot{\gamma} = 1/t)}{\eta_0} \cong \beta\gamma^{*1-\beta} \left( \frac{t}{\tau_c} \right)^{1-\beta}. \tag{48}$$

Similarly, the steady shear viscosity at high Wi for a generalized damping function of the form given in Eq. (14) [for the strong damping limit ( $m > 1 - \beta$ )] can also be approximated from Eq. (36) by substituting  $\dot{\gamma} = 1/t$  to obtain

$$\lim_{Wi/\gamma^* \gg 1} \frac{\eta(\dot{\gamma} = 1/t)}{\eta_0} \cong \frac{\pi\beta\gamma^{*1-\beta}}{m\Gamma(1-\beta)\sin\left[\frac{\pi(1-\beta)}{m}\right]} \left( \frac{t}{\tau_c} \right)^{1-\beta}. \tag{49}$$

Comparing Eq. (46) with Eqs. (48) and (49), we can see that the exponent characterizing the growth in time of the transient viscosity at short times is  $1 - \beta$  and is equal to the exponent characterizing the rate-dependence of the steady shear viscosity at high shear rates (where  $\dot{\gamma} = 1/t$ ), provided the damping is sufficiently strong. Equating the expressions for the front factors in these equations leads to Eq. (43).

This asymptotic analysis shows that, similar to the conditions derived for the Cox–Merz rule, the Gleissle mirror relation is also expected to hold to within a constant numerical factor for sufficiently strong damping forms. However, from Eq. (38), we can note that the exponent characterizing the rate-dependence of the steady shear viscosity at high Wi is not  $(1 - \beta)$  [since  $\eta(\dot{\gamma}) \sim \dot{\gamma}^{-m}$  in the case of weak damping] and hence the Gleissle mirror relation does not hold true in the weak damping limit. Having the same condition (i.e., the need for strong damping) for both the Cox–Merz rule and the Gleissle mirror relation allows experimentalists to combine the Cox–Merz rule and the Gleissle mirror relation in order to interconvert at will between the linear viscoelastic envelope defined by the transient viscosity  $\eta^+(t)$ , the complex viscosity  $|\eta^*(\omega)|$ , and the steady shear viscosity  $\eta(\dot{\gamma})$ . This combination of the Cox–Merz rule and the Gleissle mirror relationship has been used by Yan *et al.*<sup>63</sup> to combine data for polystyrene melts.

As we noted earlier, the “mirror” name comes from the fact that the exponent characterizing the dependence of the transient viscosity with time is a reflection (on logarithmic axes) of the dependence of the steady shear viscosity on shear rate as we have illustrated graphically in Figs. 6(a) and 6(b) for the FML model. When reflected using the mapping  $\dot{\gamma} = 1/t$ , high values of the Weissenberg number

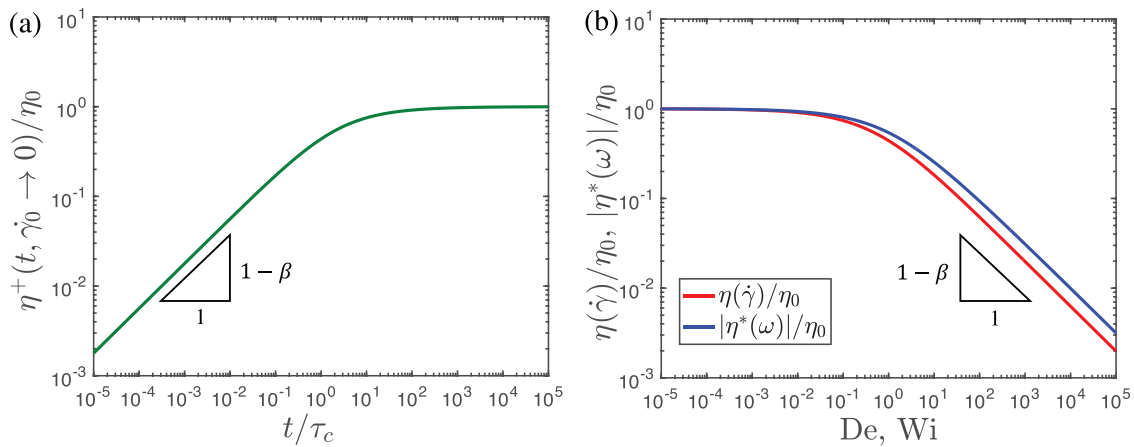


**FIG. 6.** (a) The transient viscosity for the FML model evaluated from Eq. (44) for  $\beta = 0.5$ . (b) A comparison of the complex viscosity and the steady shear viscosity predicted when Eq. (43) is satisfied. Here, the model values used are  $\beta = 0.5$ ,  $\gamma^* = 0.8$ , and  $m = 2$ .

( $Wi = \tau_c \dot{\gamma} \gg 1$ ) thus correspond to the linear viscoelastic response at early times,  $\tau_c/t \gg 1$  (or, equivalently  $t/\tau_c \ll 1$ ). Similarly, the steady shear viscosity measured at low  $Wi$  values ( $Wi = \tau_c \dot{\gamma} \ll 1$ ) will correspond to the linear viscoelastic response at long times,  $\tau_c/t \ll 1$  (or, equivalently  $t/\tau_c \gg 1$ ).

When the Gleissle mirror relation is satisfied, we can also note from Eqs. (43) and (41) that at high values of  $De$  (or  $\tau_c/t \gg 1$ ) the complex viscosity is always slightly greater than the transient viscosity  $\eta^+(t)$ —when reflected and plotted vs  $\tau_c/t$ —because  $\beta/\Gamma(2-\beta) < 1 \forall 0 \leq \beta < 1$ . A comparison between the reflected transient viscosity  $\eta^+(t)$  (plotted as a function of  $\tau_c/t$ ), the complex viscosity, and the steady shear viscosity is illustrated in Fig. 7 for the case when the Gleissle mirror relation is identically satisfied [i.e., when Eq. (43) is satisfied].

Finally, we show experimental data obtained for the 8% alginate solution in Fig. 8(a). The transient viscosity corresponding to start-up of steady shear flow at a low shear rate  $\dot{\gamma}_0 = 0.02 \text{ s}^{-1}$  (corresponding to  $Wi = 0.0013$ ) is compared with the FML prediction (with no adjustable parameters) obtained by evaluating Eq. (45) using the parameters given in Fig. 5. The power-law growth in the viscosity at short times is evident and the quantitative agreement between the FML model prediction and the measured data is excellent. In Fig. 8(b), we reflect these data (and the model prediction) using the Gleissle mirror relationship (i.e., mapping  $t \rightarrow 1/\dot{\gamma}$ ). We also present the measured complex and steady shear viscosity again to clearly illustrate the mirror-like relationship between the steady shear viscosity and the transient viscosity function that is measured at low shear rates. In contrast to Fig. 7, the reflected transient viscosity data do not overlay *exactly* on the steady shear viscosity because the numerical values of  $m$ ,  $\gamma^*$ , and  $\beta$  characterizing the alginate solution do not exactly satisfy Eq. (43) but satisfy Eq. (41) more closely.

This reflective quality, although perhaps puzzling from an experimental viewpoint, arises naturally in the integral framework employed in the present work. This is because of the nature of the damping function and the limits of the integrals in expressions such as Eq. (16) which

cut off contributions from parts of the linear viscoelastic spectrum beyond an upper limit that depends on the quantity  $Wi/\gamma^*$ , and thus provide a direct connection to definite integrals such as Eq. (45).

**V. CONCLUSION**

In this work, we have derived mathematical expressions for the steady shear viscosity, the complex viscosity and the transient (start-up) viscosity for a Wagner integral constitutive formulation with a fractional Maxwell kernel that compactly describes a complex fluid with a broad spectrum of relaxation times. The resulting integral, Eq. (4), is a simplification of the time-strain separable K-BKZ constitutive equation that can capture many different forms of the relaxation

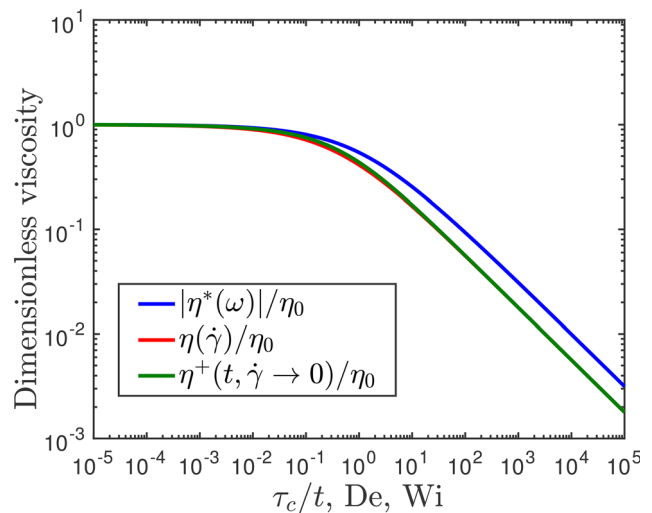


**FIG. 7.** Intercomparison of the transient viscosity  $\eta^+$  (plotted against  $\tau_c/t$ ), the complex viscosity  $|\eta^*(\omega)|$ , and the steady shear viscosity when Eq. (43) is satisfied. Here, the model parameters used are  $\beta = 0.5$ ,  $\gamma^* = 0.8$ , and  $m = 2$ .

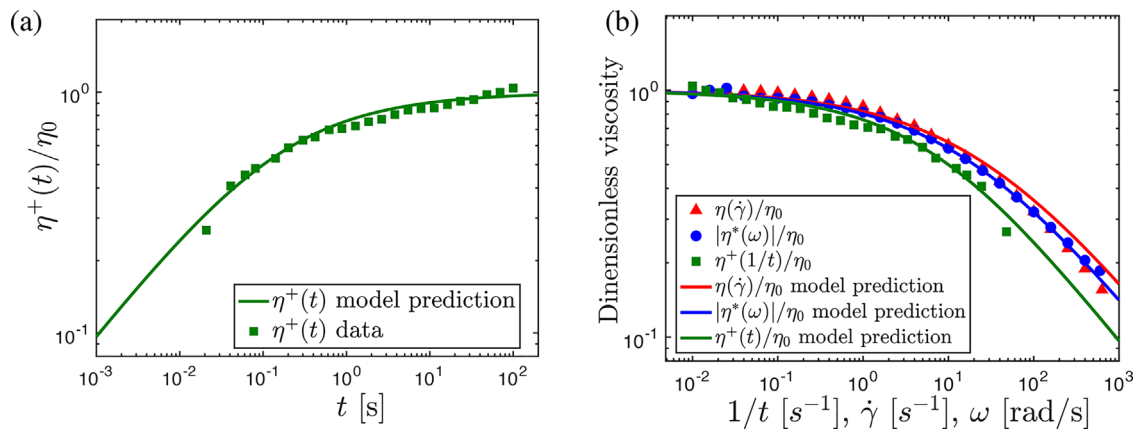


**FIG. 8.** (a) Measured values of the transient viscosity at  $\dot{\gamma}_0 = 0.02 \text{ s}^{-1}$  of the 8% alginate solution are represented by data points and the FML prediction from Eq. (45) is illustrated by the solid line. (b) Comparison of the reflected transient viscosity, complex viscosity, and the steady shear viscosity of 8% alginate solution. The solid lines represent the model predictions. The model parameter values are obtained from Fig. 5 and are  $m = 1.4$ ,  $\gamma^* = 2.5$ ,  $\beta = 0.56$ ,  $\eta_0 = 7 \text{ Pa s}$ , and  $G = 23 \text{ Pa s}^\beta$ .

spectrum, as well as different strain-dependent damping responses, corresponding to what we have identified as *weak* and *strong* damping limits. From the resulting expressions, we can summarize the following key points:

- Empirical relations such as the Cox–Merz rule do not generally hold true for materials exhibiting a narrow relaxation spectrum characterized by a single relaxation time.
- The Cox–Merz rule as well as the Gleissle mirror relationship will always hold true, to within a constant numerical factor of order unity, for viscoelastic materials exhibiting broad relaxation spectra and sufficiently strong strain-softening that can be characterized by an exponential damping function or a generalized form of Soskey–Winter damping [as given by Eq. (14)] with  $m \geq 1 - \beta$ .
- Neither the Cox–Merz rule nor the Gleissle mirror relationship is satisfied for materials exhibiting broad relaxation spectra and weak strain-dependent damping or softening such as the generalized damping given by Eq. (14) with  $m < 1 - \beta$ .

Because the exponent in the fractional Maxwell model is always limited to  $\beta < 1$ , the constraint we have identified above as *strong damping* (i.e.,  $m \geq 1 - \beta$ ) is, in fact, not very restrictive at all. For example, the Doi–Edwards damping function corresponds to  $m = 2$  and so satisfies this constraint for a wide range of viscoelastic materials in which the relaxation spectrum is of Rouse ( $\beta = 0.5$ ) or Zimm ( $\beta = 0.66$ ) form. This probably explains why these empirical rules apply so broadly to many polymeric systems.<sup>16</sup> It is also commonly observed that the critical strain  $\gamma^*$  in many polymeric complex fluids is of order unity. Under such conditions, we have shown from our analysis and the plots in Fig. 4 that we should expect the magnitude of the complex viscosity to be slightly greater than the steady shear viscosity at high Wi and De [i.e., positive contour values in Fig. 4(a)]. This is in agreement with the most commonly observed deviations from the Cox–Merz rule reported by Vlassopoulos and coworkers.<sup>16</sup> However, they also note that in some highly branched polymer systems precise measurements can show that  $|\eta^*(\omega)| < \eta(\dot{\gamma})$  at high Wi or De.

Careful inspection of Fig. 4(a) shows that our analysis also predicts a small region at high Wi (between the dashed and solid lines) where *strong* damping (and thus good agreement with the Cox–Merz rule) is still observed but the ratio of viscosities is less than unity. The values of  $m \simeq 0.9$  in this region correspond to the damping function for a transient polymer network with relatively little strain-softening, as would be expected for highly branched materials.

There appear to be very few materials that fall into the *weak* damping limit ( $m < 1 - \beta$ ). However, one class of systems are bread doughs, which—due to hydrogen-bonding between gluten molecules—form highly viscoelastic network-like materials that only strain-soften very slightly, even up to high strains. They thus exhibit an almost (but not quite) neo-Hookean response with weak strain-softening.<sup>64</sup>

Interestingly, the key numerical conditions that we derive for satisfying the Cox–Merz rule [Eq. (41)] and the Gleissle mirror rule [Eq. (43)] cannot both be satisfied identically, because the function on the right-hand side of Eq. (43) has a value  $\beta/\Gamma(2 - \beta) < 1$  for  $\beta < 1$ . However, the actual numerical difference between these expressions is small for most values of  $\beta$  (specifically, the difference is less than a factor of two for  $0.5 \leq \beta < 1$ ). On a double logarithmic plot such as Fig. 8, the difference is very small when  $\beta = 0.56$ .

Although our analysis of these empirical relationships has been based on continuum mechanics, we can also make connections to the underlying mechanisms that are proposed to be important in microscopic theories. Marrucci<sup>65</sup> considered the impact of convective constraint release (CCR) on entanglement dynamics at high shear rates and derived a non-integer power-law expression for rate-thinning in the steady shear viscosity of entangled melts that are characterized by a broad relaxation spectrum (specifically the Rouse spectrum corresponding to  $\beta = 0.5$ ). By comparing the model predictions with the analytic expression for the frequency dependence of the complex viscosity of a Rouse chain, good agreement with the Cox–Merz rule (to within a numerical constant of order unity) at high shear rates and frequencies was demonstrated. Our continuum mechanics-based approach does not explicitly incorporate microscopic mechanisms such as CCR but is

consistent with the analysis of Marrucci; his incorporation of convective constraint release into a rate-dependent relaxation time effectively reduces the characteristic time scale for stress relaxation at high shear rates, in much the same way that a strong decrease in the damping function does. Our analysis further shows that the Cox–Merz rule will also be satisfied (in the limit of strong damping) for a wide selection of other discrete or continuous relaxation spectra (beyond just the Rouse spectrum that fixes  $\beta = 0.5$ ) provided that they are of Rouse–Zimm form and give  $G(t) \sim t^{-\beta}$  at short times.

Mead, Larson, and Doi<sup>66</sup> incorporated CCR into the Doi–Edwards–Marrucci–Grizzuti (DEMG) theory and derived a multiplicative correction factor to the Doi–Edwards (DE) strain-dependent damping function. This extended model is now commonly referred to as the Mead–Larson–Doi (MLD) model. The correction factor in the MLD model amplifies strain-softening at large strain amplitudes; however, the DE damping function by itself is already a “strong” damping function by our definition ( $m = 2$ ), as discussed in Sec. IV. Therefore, the validity of the Cox–Merz rule for the MLD model reported in Ref. 67 is again consistent with the strong damping condition that we have derived from our continuum mechanics analysis.

Finally, we note that the “shear blob” kinetic theory model introduced by Rabin and Ottinger<sup>68</sup> also aims to capture shear thinning in polymer solutions through the effects of internal viscosity. They develop an expression for the shear-induced evolution of the relaxation spectrum as internal dissipation in each shear blob becomes increasingly important. The resulting relaxation spectrum becomes a function of a “generalized Weissenberg number” and interpolates smoothly between the zero-frequency and high-frequency limits of a bead-spring chain. They note that in strong deformations, relaxation processes in the chain are dominated by internal modes with time scales shorter than  $\tau \sim \dot{\gamma}^{-1}$ . This is exactly analogous to the varying cutoffs in the integrals we analyze in Eqs. (16), (45), and (48). The combination of a broad relaxation spectrum and a rate-dependent cutoff again results in a model that satisfies the Cox–Merz rule and the Gleissle mirror relationship, and this is again consistent with our general continuum analysis.

The interplay between constitutive modeling, mathematical analysis, and experimental data represented in this paper is inspired by the same considerations that permeate Bob Bird’s extensive contributions to our subject. We hope that the results we have derived here provide a better understanding of why these useful empirical rules work and why they are so widely used throughout the complex fluids community.

**ACKNOWLEDGMENTS**

J.D.J.R. would like to thank Aramco Americas for financial support of his studies on non-linear viscoelastic materials. G.H.M. and B.K. would like to thank P&G for a gift to support work in the Non-Newtonian Fluids group as well as Dr. W. Hartt and Professor D. Vlassopoulos for motivating and insightful discussions.

**AUTHOR DECLARATIONS**

**Conflict of Interest**

The authors have no conflicts to disclose.

**DATA AVAILABILITY**

The data that support the findings of this study are available from the corresponding author upon reasonable request.

**APPENDIX: COX–MERZ RULE FOR POLYSTYRENE MELTS OF VARYING TOPOLOGY**

As we have shown in the main text in Eq. (41), we need the following condition to be satisfied for the Cox–Merz rule to be identically valid:

$$f = \frac{\pi\beta(\gamma^*)^{1-\beta}}{m\Gamma(1-\beta)\sin\left[\frac{\pi(1-\beta)}{m}\right]} = 1. \tag{A1}$$

Therefore, one can determine *a priori* by evaluating the numerical value of  $f$  whether a given complex fluid is expected to satisfy the Cox–Merz rule. This requires values of the damping function parameters ( $m$  and  $\gamma^*$ ) and the exponent  $\beta$  characterizing the time-dependent decay in the relaxation modulus [ $G(t) \sim t^{-\beta}$ ] at short times (or the power-law dependency of the complex modulus at high frequencies). If the value of  $f$  is close to unity, it indicates that the Cox–Merz rule will be satisfied and thus allow for interconversion between the steady shear viscosity and the complex viscosity.

Here, we apply this analysis to data obtained by Vlassopoulos and coworkers for melts of linear polystyrene chains (PS-84k linear) and polystyrene rings (PS-84k ring). The parameters characterizing the damping function for the PS-84k linear chains and PS-84k rings at  $T = 150^\circ\text{C}$  are obtained from Ref. 63. Similarly, the power-law exponent  $\beta$  characterizing the relaxation modulus at short times for the PS-84k linear chains and PS-84k rings at  $T = 150^\circ\text{C}$  are obtained from Ref. 69. We fit the Soskey–Winter damping function [Eq. (14)] to the measurements of  $h(\gamma)$  as shown in Fig. 9. The resulting fit is extremely good for both systems. The Soskey–Winter damping function also accurately describes additional data provided by the authors for blends of rings and chains; but these data are not shown here for clarity. Both melts correspond to the strong damping limit with  $m > 1 - \beta$  and we further note that the melt of

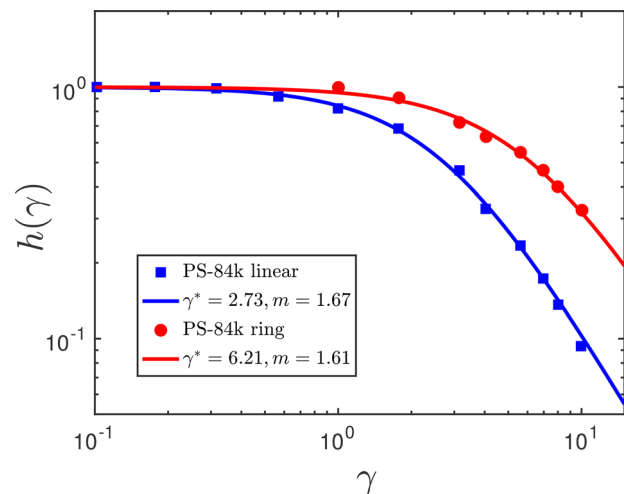


**FIG. 9.** Measurement values of the damping function for melts of linear polystyrene chains as well as for entangled rings of the same molecular weight at  $T = 150^\circ\text{C}$  from Ref. 63. The general Soskey–Winter damping functional form in Eq. (14) provides a good fit to both sets of data as shown by the solid lines.

**TABLE III.** Values of the two model parameters for the general damping function fit ( $m$  and  $\gamma^*$ ) and the linear FML parameter  $\beta$  [characterizing the  $G(t) \sim t^{-\beta}$  decay in the relaxation modulus at short times] for the two polystyrene melts shown in Fig. 9. The power-law exponent  $\beta$  is determined from the data shown in Fig. 2 of Parisi *et al.*<sup>69</sup>

Polymer	$\beta$	$\gamma^*$	$m$	$f$
PS-84k ring	0.61	6.21	1.61	1.54
PS-84k linear	0.29	2.73	1.67	0.89

entangled PS rings shows a significantly larger value of  $\gamma^*$ . The two parameters ( $m, \gamma^*$ ) characterizing the measurements of  $h(\gamma)$  the linear FML parameter  $\beta$  and the numerical value of our criterion  $f$  given in Eq. (A1) are tabulated in Table III.

From Table III, we find the numerical value of  $f$  evaluated from Eq. (A1) to be close to unity for both the linear and ring samples. The two systems deviate from the exact criteria of  $f=1$  by a maximum of 11% and 54%, respectively. However, even a factor of 1.54 is small when viscosity measurements are plotted on double logarithmic scales, and falls within the reported variability. This helps rationalize the excellent agreement with the Cox–Merz rule for the 84k linear and ring polystyrene melts illustrated in the paper by Parisi *et al.*<sup>69</sup>

## REFERENCES

- W. Cox and E. Merz, "Correlation of dynamic and steady flow viscosities," *J. Polym. Sci.* **28**, 619–622 (1958).
- H. C. Booij, P. Leblans, J. Palmen, and G. Tiemersma-Thoone, "Nonlinear viscoelasticity and the Cox–Merz relations for polymeric fluids," *J. Polym. Sci.: Polym. Phys. Ed.* **21**, 1703–1711 (1983).
- V. Sharma and G. H. McKinley, "An intriguing empirical rule for computing the first normal stress difference from steady shear viscosity data for concentrated polymer solutions and melts," *Rheol. Acta* **51**, 487–495 (2012).
- W. Gleissle, "Two simple time-shear rate relations combining viscosity and first normal stress coefficient in the linear and non-linear flow range," *Rheology* (Springer, 1980), pp. 457–462.
- H. M. Laun, "Prediction of elastic strains of polymer melts in shear and elongation," *J. Rheol.* **30**, 459–501 (1986).
- W.-M. Kulicke and R. S. Porter, "Relation between steady shear flow and dynamic rheology," *Rheol. Acta* **19**, 601–605 (1980).
- H. H. Winter, "Three views of viscoelasticity for Cox–Merz materials," *Rheol. Acta* **48**, 241–243 (2009).
- T. Chen, M. Q. Ansari, and D. G. Baird, "The rheology of ultra-high molecular weight poly (ethylene oxide) dispersed in a low molecular weight carrier," *Phys. Fluids* **34**, 023304 (2022).
- T. S. R. Al-Hadithi, H. A. Barnes, and K. Walters, "The relationship between the linear (oscillatory) and nonlinear (steady-state) flow properties of a series of polymer and colloidal systems," *Colloid Polym. Sci.* **270**, 40–46 (1992).
- K. Yasuda, R. C. Armstrong, and R. E. Cohen, "Shear flow properties of concentrated solutions of linear and star branched polystyrenes," *Rheol. Acta* **20**, 163–178 (1981).
- A. Jaishankar and G. H. McKinley, "A fractional K-BKZ constitutive formulation for describing the nonlinear rheology of multiscale complex fluids," *J. Rheol.* **58**, 1751–1788 (2014).
- D. Doraiswamy, A. N. Mujumdar, I. Tsao, A. N. Beris, S. C. Danforth, and A. B. Metzner, "The Cox–Merz rule extended: A rheological model for concentrated suspensions and other materials with a yield stress," *J. Rheol.* **35**, 647–685 (1991).
- C. Yu and S. Gunasekaran, "Correlation of dynamic and steady flow viscosities of food materials," *Appl. Rheol.* **11**, 134–140 (2001).
- A. N. Mujumdar, A. N. Beris, and A. B. Metzner, "Transient phenomena in thixotropic systems," *J. Non-Newtonian Fluid Mech.* **102**, 157–178 (2002).
- R. B. Bird, R. C. Armstrong, and O. Hassager, *Dynamics of Polymeric Liquids*, Volume 1: Fluid Mechanics (Wiley, 1987).
- F. Sniijkers and D. Vlassopoulos, "Appraisal of the Cox–Merz rule for well-characterized entangled linear and branched polymers," *Rheol. Acta* **53**, 935–946 (2014).
- J. M. Dealy, "Weissenberg and Deborah numbers their definition and use," *Rheol. Bull.* **79**, 14–18 (2010).
- C. Saengow and A. J. Giacomin, "Exact solutions for oscillatory shear sweep behaviors of complex fluids from the Oldroyd 8-constant framework," *Phys. Fluids* **30**, 030703 (2018).
- A. C. Pipkin, *Lectures on Viscoelasticity Theory* (Springer Science and Business Media, 2012), Vol. 7.
- R. H. Ewoldt and G. H. McKinley, "Mapping thixo-elasto-visco-plastic behavior," *Rheol. Acta* **56**, 195–210 (2017).
- R. G. Larson, *Constitutive Equations for Polymer Melts and Solutions*, Butterworths Series in Chemical Engineering (Butterworth-Heinemann, 2013).
- M. H. Wagner, "Analysis of time-dependent non-linear stress-growth data for shear and elongational flow of a low-density branched polyethylene melt," *Rheol. Acta* **15**, 136–142 (1976).
- V. H. Rolon-Garrido and M. H. Wagner, "The damping function in rheology," *Rheol. Acta* **48**, 245–284 (2009).
- R. I. Tanner, "From A to (BK) Z in constitutive relations," *J. Rheol.* **32**, 673–702 (1988).
- N. Ghahramani, K. A. Iyer, A. K. Doufas, and S. G. Hatzikiriakos, "Rheological modeling of thermoplastic vulcanizates (TPVs) using the Kaye–Bernstein, Kearsley, Zapas (K–BKZ) constitutive law," *Phys. Fluids* **33**, 083107 (2021).
- D. J. Curtis and A. R. Davies, "On response spectra and Kramers-Kronig relations in superposition rheometry," *Phys. Fluids* **31**, 127105 (2019).
- M. Ebrahimi, V. K. Konaganti, and S. G. Hatzikiriakos, "Dynamic slip of poly-disperse linear polymers using partitioned plate," *Phys. Fluids* **30**, 030601 (2018).
- R. G. Larson, "Constitutive relationships for polymeric materials with power-law distributions of relaxation times," *Rheol. Acta* **24**, 327–334 (1985).
- H. H. Winter, "The critical gel," *Structure and Dynamics of Polymer and Colloidal Systems* (Springer, 2002), pp. 439–470.
- M. Renardy, "Qualitative correlation between viscometric and linear viscoelastic functions," *J. Non-Newtonian Fluid Mech.* **68**, 133–135 (1997).
- P. J. R. Leblans, J. Samper, and H. C. Booij, "The mirror relations and nonlinear viscoelasticity of polymer melts," *Rheol. Acta* **24**, 152–158 (1985).
- R. S. Rivlin and K. N. Sawyers, "Nonlinear continuum mechanics of viscoelastic fluids," *Annu. Rev. Fluid Mech.* **3**, 117–146 (1971).
- M. H. Wagner, "Damping functions and nonlinear viscoelasticity—A review," *J. Non-Newtonian Fluid Mech.* **68**, 169–171 (1997).
- P. R. Soskey and H. H. Winter, "Large step shear strain experiments with parallel-disk rotational rheometers," *J. Rheol.* **28**, 625–645 (1984).
- W. H. Li, H. Du, G. Chen, S. H. Yeo, and N. Q. Guo, "Nonlinear rheological behavior of magnetorheological fluids: Step-strain experiments," *Smart Mater. Struct.* **11**, 209 (2002).
- M. Iza and M. Bousmina, "Nonlinear rheology of immiscible polymer blends: Step strain experiments," *J. Rheol.* **44**, 1363–1384 (2000).
- C. Valencia, M. C. Sanchez, A. Ciruelos, A. Latorre, J. M. Madiedo, and C. Gallegos, "Non-linear viscoelasticity modeling of tomato paste products," *Food Res. Int.* **36**, 911–919 (2003).
- M. Oblonšek, S. Šostar-Turk, and R. Lapasin, "Rheological studies of concentrated guar gum," *Rheol. Acta* **42**, 491–499 (2003).
- P. R. Soskey and H. H. Winter, "Equibiaxial extension of two polymer melts: Polystyrene and low density polyethylene," *J. Rheol.* **29**, 493–517 (1985).
- J. D. J. Rathinaraj, G. H. McKinley, and B. Keshavarz, "Incorporating rheological nonlinearity into fractional calculus descriptions of fractal matter and multi-scale complex fluids," *Fractal Fract.* **5**, 174 (2021).
- M. H. Wagner and J. Meissner, "Network disentanglement and time-dependent flow behaviour of polymer melts," *Die Makromol. Chem.: Macromol. Chem. Phys.* **181**, 1533–1550 (1980).



- <sup>42</sup>The upper incomplete Gamma function has the following asymptotic limits: (i) For  $m < 2$ ,  $\lim_{x \rightarrow 0} \Gamma_u(2 - m, x) = \Gamma(2 - m)$  and (ii) for  $m \geq 2$ ,  $\lim_{x \rightarrow 0} \Gamma_u(2 - m, x) \sim x^{2-m}$ .
- <sup>43</sup>There is one special case, when  $m = 1$  and  $\gamma^* = 1$  for which the Cox–Merz relationship would be satisfied in a fluid with a linear viscoelastic response that is characterized by a single mode Maxwell model. In principle, this might be achievable, for example, in a worm-like micellar fluid in which the strain damping function is engineered (e.g., by adjusting the salt concentration) to be described by Eq. (14) with  $m = 1$ , but we are unaware of a physical embodiment that accurately satisfies this constraint.
- <sup>44</sup>A. Lion, “On the thermodynamics of fractional damping elements,” *Continuum Mech. Thermodyn.* **9**, 83–96 (1997).
- <sup>45</sup>R. L. Bagley and P. Torvik, “A theoretical basis for the application of fractional calculus to viscoelasticity,” *J. Rheol.* **27**, 201–210 (1983).
- <sup>46</sup>R. L. Bagley and P. J. Torvik, “On the fractional calculus model of viscoelastic behavior,” *J. Rheol.* **30**, 133–155 (1986).
- <sup>47</sup>A. Jaishankar and G. H. McKinley, “Power-law rheology in the bulk and at the interface: Quasi-properties and fractional constitutive equations,” *Proc. R. Soc. A* **469**, 20120284 (2013).
- <sup>48</sup>H. Schiessel, R. Metzler, A. Blumen, and T. F. Nonnenmacher, “Generalized viscoelastic models: Their fractional equations with solutions,” *J. Phys. A: Math. Gen.* **28**, 6567 (1995).
- <sup>49</sup>I. Podlubny, *Fractional Differential Equations: An Introduction to Fractional Derivatives, Fractional Differential Equations, to Methods of their Solution and Some of their Applications* (Elsevier, 1998).
- <sup>50</sup>K. Adolphsson, M. Enelund, and P. Olsson, “On the fractional order model of viscoelasticity,” *Mech. Time-Depend. Mater.* **9**, 15–34 (2005).
- <sup>51</sup>M. Enelund and G. A. Lesiute, “Time domain modeling of damping using an elastic displacement fields and fractional calculus,” *Int. J. Solids Struct.* **36**, 4447–4472 (1999).
- <sup>52</sup>N. W. Tschoegl, *The Phenomenological Theory of Linear Viscoelastic Behavior: An Introduction* (Springer-Verlag, Berlin, Heidelberg, 1989).
- <sup>53</sup>L.-I. Palade, V. Verney, and P. Attané, “A modified fractional model to describe the entire viscoelastic behavior of polybutadienes from flow to glassy regime,” *Rheol. Acta* **35**, 265–273 (1996).
- <sup>54</sup>K. Sadman, Q. Wang, Y. Chen, B. Keshavarz, Z. Jiang, and K. R. Shull, “Influence of hydrophobicity on polyelectrolyte complexation,” *Macromolecules* **50**, 9417–9426 (2017).
- <sup>55</sup>L. Martinetti and R. H. Ewoldt, “Time-strain separability in medium-amplitude oscillatory shear,” *Phys. Fluids* **31**, 021213 (2019).
- <sup>56</sup>K. Yasuda, “Investigation of the analogies between viscometric and linear viscoelastic properties of polystyrene fluids,” Ph.D. thesis (Massachusetts Institute of Technology, 1979).
- <sup>57</sup>P. J. Carreau, “Rheological equations of state from molecular network theories,” Ph.D. thesis (University of Wisconsin, Madison, 1968).
- <sup>58</sup>O. Manero, F. Bautista, J. F. A. Soltero, and J. E. Puig, “Dynamics of worm-like micelles: The Cox–Merz rule,” *J. Non-Newtonian Fluid Mech.* **106**, 1–15 (2002).
- <sup>59</sup>J. D. J. Rathinaraj, J. Hendricks, G. H. McKinley, and C. Clasen, “Orthochirp: A fast spectro-mechanical probe for monitoring transient microstructural evolution of complex fluids during shear,” *J. Non-Newtonian Fluid Mech.* **301**, 104744 (2022).
- <sup>60</sup>H. B. Eral, E. R. Safai, B. Keshavarz, J. J. Kim, J. Lee, and P. Doyle, “Governing principles of alginate microparticle synthesis with centrifugal forces,” *Langmuir* **32**, 7198–7209 (2016).
- <sup>61</sup>W. Gleissle and B. Hochstein, “Validity of the Cox–Merz rule for concentrated suspensions,” *J. Rheol.* **47**, 897–910 (2003).
- <sup>62</sup>The Mittag–Leffler function  $E_{a,b}(z)$  for  $z \ll 1$  can be approximated as  $E_{a,b}(z) = \sum_{k=1}^N \frac{z^{k-1}}{\Gamma(a(k-1)+b)} + \mathcal{O}(z^{N+1})$  and hence can be approximated to the leading term  $1/\Gamma(b) + \mathcal{O}(z^1)$  for  $z \ll 1$ .
- <sup>63</sup>Z.-C. Yan, S. Costanzo, Y. Jeong, T. Chang, and D. Vlassopoulos, “Linear and nonlinear shear rheology of a marginally entangled ring polymer,” *Macromolecules* **49**, 1444–1453 (2016).
- <sup>64</sup>Y. Meeus, M. Meerts, D. Szilvási, G. H. McKinley, R. Cardinaels, and P. Moldenaers, “Extensional stress-relaxation measurements on wheat flour dough—the key to finalizing the fractional K-BKZ framework?,” in Proceedings of the 92nd Annual Meeting of the Society of Rheology, 10–14 October 2021, Bangor, Maine (2021).
- <sup>65</sup>G. Marrucci, “Dynamics of entanglements: A nonlinear model consistent with the Cox–Merz rule,” *J. Non-Newtonian Fluid Mech.* **62**, 279–289 (1996).
- <sup>66</sup>D. W. Mead, R. G. Larson, and M. Doi, “A molecular theory for fast flows of entangled polymers,” *Macromolecules* **31**, 7895–7914 (1998).
- <sup>67</sup>D. W. Mead, “Analytic derivation of the Cox–Merz rule using the MLD toy model for polydisperse linear polymers,” *Rheol. Acta* **50**, 837–866 (2011).
- <sup>68</sup>Y. Rabin and H. C. Öttinger, “Dilute polymer solutions: Internal viscosity, dynamic scaling, shear thinning and frequency-dependent viscosity,” *Europhys. Lett.* **13**, 423 (1990).
- <sup>69</sup>D. Parisi, S. Costanzo, Y. Jeong, J. Ahn, T. Chang, D. Vlassopoulos, J. D. Halverson, K. Kremer, T. Ge, M. Rubinstein *et al.*, “Nonlinear shear rheology of entangled polymer rings,” *Macromolecules* **54**, 2811–2827 (2021).